Chapter 6
Ceramics, Marbles and Stones in the Light of Neutrons: Characterization by Various Neutron Methods

Zsolt Kasztovszky, Veronika Szilágyi, Katalin T. Biró, Judit Zöldföldi, M. Isabel Dias, António Valera, Emmanuel Abraham, Maryelle Bessou, Fabrizio LoCelso and Valerio Benfante

Abstract In this chapter we give a brief overview of neutron based analytical investigations applied to study archaeological ceramics, and different types of stones. Since the vast majority of archaeological objects are made of ceramics and various stones—all are of geological origin—, one of the key objectives of these studies to determine the origin of raw material. This research is called provenance

Zs. Kasztovszky (✉) · V. Szilágyi
Centre for Energy Research, Hungarian Academy of Sciences,
H-1121 Konkoly-Thege str. 29-33, Budapest, Hungary
e-mail: kasztovszky.zsolt@energia.mta.hu

V. Szilágyi
e-mail: szilagyi.veronika@energia.mta.hu

K.T. Biró
Hungarian National Museum, H-1088 Múzeum krt. 14-16, Budapest, Hungary
e-mail: tbk@hnm.hu

J. Zöldföldi
Institute of Materials Science, University of Stuttgart, Stuttgart, Germany
e-mail: Judit.Zoeldfoeldi@mpa.uni-stuttgart.de

M. Isabel Dias
Centro de Ciências e Tecnologias Nucleares. Campus Tecnológico e Nuclear,
Instituto Superior Técnico, Estrada Nacional 10, ao km 139,7,
2695-066 Bobadela LRS, Portugal
e-mail: isadias@ctn.tecnico.ulisboa.pt

A. Valera
Era Arqueologia, Núcleo de Investigação Arqueológica – NIA, Cç. de Santa Catarina,
9C, 1495-705 Cruz Quebrada – Dafundo, Portugal
e-mail: antoniovalera@era-arqueologia.pt

A. Valera
Interdisciplinary Center for Archaeology and Evolution of Human Behavior
(ICArHEB), Universidade do Algarve, Campo de Gambelas, Faro, Portugal

E. Abraham
University of Bordeaux, LOMA, CNRS UMR, 5798 Talence, France
e-mail: emmanuel.abraham@u-bordeaux.fr

N. Kardjilov and G. Festa (eds.), *Neutron Methods for Archaeology and Cultural Heritage*, Neutron Scattering Applications and Techniques,
DOI 10.1007/978-3-319-33163-8_6

research, and a wide range of neutron based methods are applicable in it. Following a very basic, user-oriented description of the methods, we introduce examples from our everyday practice. The examples are about provenance of prehistoric stone tools, about the sources of 4th–3rd c. B.C. millennium limestone idols found in the South of Portugal, as well as about the characterization of 15th–16th c. A.D. Inka pottery. A very unique application of combined neutron techniques was aimed to determine the inner content of an Eighteenth Dynasty Egyptian sealed vessel. In addition, investigations of samples from different epochs and characterization of marbles are presented.

6.1 Introduction

Combination of different neutron investigation methods helps to obtain detailed picture about the properties of ancient materials like marbles, ceramics and stones. Neutron activation techniques allow for detection of the chemical composition of the materials with high precision. Neutron diffraction provides information about the crystallographic structure, textures and different phases in the materials. Imaging methods show the morphology of the materials like macro porosity, inclusions and mineral distributions. The quality of marbles can be characterized by Small Angle Neutron Scattering which provides a measure about the homogeneity and the fine granular structure of the material. The arrangement of results from the different investigations and the analysis of multi-dimensional data volumes is quite demanding task requiring broad expertise and collaboration of researchers from different fields. In this chapter, examples of such multidisciplinary investigations on ancient materials are presented.

6.2 Used Experimental Methods

6.2.1 Instrumental Neutron Activation Analysis (INAA)

Historically, this was the first of the activation analytical methods, in which a few mg of the sample is irradiated in a reactor core and the induced radioactivity is measured post-irradiation. It is a destructive elemental analytical method, mostly applicable to determine the trace elements in various materials (stones, ceramics,

M. Bessou
University of Bordeaux, PACEA, CNRS UMR, 5199 Pessac, France
e-mail: maryelle.bessou@u-bordeaux.fr

F. LoCelso · V. Benfante
DiFC, University of Palermo, 90128 Palermo, Italy

metals, etc.). It is rather sensitive down to ppb or ppt level. Fingerprint-like trace element patterns (e.g. rare-earth patterns) help to identify the geographical origin of certain raw materials (called provenance analysis); it requires a 1–100 mg sample from the objects. The principle of the method is present in detail in Chap. 10.

6.2.2 Prompt Gamma Activation Analysis (PGAA)

A particular kind of Neutron Activation Analysis; the irradiation is performed at a guided external neutron beam, and the prompt- and delayed gamma photons are measured simultaneously with the irradiation. It is absolutely non-destructive, large objects can be irradiated (external beam), and in practice, no long-lived induced activity is produced. It is applicable mostly to quantify almost all the major and minor components (H, Na, K, Mg, Al, Si, Ti, Mn, Fe and Cl) and some trace elements (B is an important one, occasionally also Cr, Sc, V, Nd, Sm and Gd). PGAA is quite applicable in provenance studies of various stone objects and ceramics, too. PGAA and Instrumental Neutron Activation Analysis (INAA) are good complementary methods which allow for detection of almost every chemical element. Most of the following examples discuss PGAA measurements at Budapest Neutron Centre (BNC) and at Heinz Maier-Leibnitz Zentrum (MLZ), Garching, Germany. For detailed information related to the PGAA experimental method, please see Chap. 11.

6.2.3 Neutron Imaging (Radiography and Tomography—NR and NT)

The neutron imaging methods are rarely used to investigate homogeneous objects, like stone tools or bulky ceramics, but it can be useful to visualize the inner content of a closed vessel, or to investigate manufacturing (e.g. joins) of a ceramic vessel. One example of an Egyptian jar is discussed as an example. The NR&NT experimental methods are described in detail in Chap. 16.

6.2.4 Prompt Gamma Activation Imaging (PGAI)

PGAI is a combination of the neutron imaging methods with the elemental analysis, i.e. an extension of bulk PGAA towards the 3D elemental mapping. It is less important when investigating a homogeneous object, but is necessary to study the special distribution of various elements within inhomogeneous objects. The most important factors are the sensitivity, which is determined by nuclear constants similarly to PGAA and the spatial resolution, which is determined by the width of the neutron beam. The example of the Egyptian jar is illustrative here also. For more information about the PGAI technique, please see Chap. 14.

6.2.5 Time-of-Flight Neutron Diffraction (TOF-ND)

TOF-ND is used for exploring crystallographic phases, and other atomic-scale structural features. It can be used to identify various minerals in rocks or ceramics. From the literature, we know there was an attempt to investigate archaeological ceramics with TOF-ND. The ND method is presented in detail in Chap. 9.

6.2.6 Small Angle Neutron Scattering (SANS)

SANS is a technique for studying nanometer scale structural features in various materials. The information obtained is characteristic for the whole irradiated volume of the sample. Practically, the measured piece is free from outer-shape, physical, chemical or structural changes; there is no need of sampling. SANS makes possible the determination of void sizes in porous media, observation of typical grain sizes, anisotropy in the precipitate orientation in minerals or metals, as well as the investigation of particle agglomeration in ceramic bodies and evolution of pores during different types of processing. Detailed information about the principle of the SANS method can be found in Chap. 9.

6.3 Examples of Neutron Studies on Ceramics, Stones and Marbles

6.3.1 Provenance Studies on Prehistoric Stone Objects[1]

Lithic artefacts are among the first documented evidence of human tool use. They occur from the earliest Palaeolithic times up to modern hunter-gatherer communities of the recent past. In Hungary, the first stone implements are connected with the Vértesszőlős Lower Palaeolithic site (400,000 B.C.) and they are in use all through prehistoric times, including the Neolithic Period and also into the age of metals. On Fig. 6.1 we show a simplified chronological chart for the interior parts of the Carpathian Basin (after Biró and Regenye 1995; Visy et al. 2003).

In the Palaeolithic period, chipped stone objects were produced, e.g. blades, scrapers, projectile points; while in the Neolithic period, apart from the traditional chipped stone implements, nicely elaborated polished stone tools appeared as well. Prehistoric people were absolutely aware of the requirements for producing optimal

[1]Section written by Zsolt Kasztovszky and Katalin T. Biró.

Period	Age	Transdanubian cultures	To the East of the Danube (Alföld and North-Hungarian Mts.)	Time scale (thousand years)
Historical periods		Pannonia (Roman Empire)	Barbaricum	2
Prehistoric period	Iron Age	Celts Halstatt culture	Scythians Prescythian culture	3
	Bronze Age	Urngrave culture Mouldgrave culture Incrusted ware culture	Gáva culture Füzesabony culture Nyírség culture	4
	Copper Age	Baden culture Balaton-Lasinja culture	Baden culture Bodrogkeresztúr c. Tiszapolgár culture	5
	Neolithic = New Stone Age	Lengyel culture Linearband pottery culture Starčevo culture	Tisza culture Linearband pottery culture Körös culture	6 8
Mesolithic period		?	Jászság group	10
Palaeolithic period	Upper Pal. Middle Pal. Lower Pal.	Gravettian culture Jankovichian culture Mousterian culture Buda industry (= Vértesszölös)	Gravettian culture Szeletian culture Aurignacian culture Mousterian culture	18 30 50 500

Fig. 6.1 Simplified chronological chart for the interior parts of the Carpathian Basin (after Biró and Regenye 1995; Visy et al. 2003). The time scale indicates thousand years before present (B.P.)

stone tools and the localities of occurrence for good quality raw materials. The locations and quality of different rocks, such as obsidian, flint, radiolarite, silex, porphyry and metamorphic rocks (greenschist, blueschist, serpentinite, nefrite, etc.) are primarily determined by geological factors. These factors are embedded as signals in the raw materials proper. In other words, their geochemical composition is very often 'fingerprint-like', i.e., characteristic for the provenance of the raw material used for lithic artefacts.

One of the key questions for archaeometry is to find the provenance (place of origin, the geological source) of the archaeological objects found in controlled and documented context on the archaeological sites. If we are able to identify and quantitatively measure characteristic features (isotopic, elemental or mineralogical composition of the artefacts), we might have a chance to provide data about the geographical distribution of different raw materials, as transported by prehistoric people by means of regional supply systems or occasionally long distance trade networks.

Obsidian is a homogeneous type of natural (volcanic) glass. It has perfect conchoidal fracture, is easy to work on with simple percussion techniques, yielding very sharp cutting edges. Though it is as brittle as any glass, obsidian is hard enough for regular use. Because of its attractive appearance and advantageous mechanical qualities, it was a popular raw material during prehistory. The formation of obsidian requires the co-existence of specific geological conditions. It is formed when the fluid volcanic melt meets seawater or ice and quickly solidifies. This process is known as quenching. However, not every volcanic glass is regarded as obsidian; it requires rhyolitic lava with a very high SiO_2 content and a low amount of volatiles, especially water.

Because of the very specific geological conditions of obsidian formation, the major obsidian sources are quite well known. One can find obsidian all over the world along young volcanic insular arches, in New Zealand, the Andes or in Japan. In Europe and the Near East, the most important sources can be found in the Mediterranean region (Sardinia, Lipari, Melos and Anatolia). Most of the obsidian sources are geologically very young since glass is typically not stable under normal surface conditions. The Central European obsidian sources are relatively old, formed in the Tertiary period. The sources are mainly located in the Tokaj-Eperjes Mountains, at the border of today's Hungary and Slovakia. Further obsidian occurrences are known from Transcarpathian Ukraine in the environs of Huszt around Rokosovo. The Central European obsidian sources are generally referred to, in archaeometrical technical literature, as 'Carpathian' obsidian, though this term is incorrect from a geographical or geological aspect.

Fortunately, the geochemical (elemental) compositions of various obsidians are very characteristic for the conditions of the formation, and hence for the place of geological origin. The first research on archaeological obsidian with the support of geological methods was started as early as in the 1860s in Hungary, in the pioneering works of Rómer (1867) and Szabó (1867), respectively. From the late 1960s, modern analytical methods have been gradually introduced to determine the geochemical properties of obsidians of different origin. Besides more or less simple spectroscopic methods such as Optical Emission Spectroscopy (OES) (Cann and Renfrew 1964), the methods of Instrumental Neutron Activation Analysis (INAA) (Oddone et al. 1999), X-ray Fluorescence Spectroscopy (XRF) (Tykot 1997) and also ion-beam analytical (PIXE, PIGE) methods (Bourdonnec et al. 2005) have been applied to quantify the amount of characteristic major-, minor- and trace elements. Although many of the above mentioned methods proved to be successful in determination of fingerprint-like trace elements, like Rb, Sr, Nb, Y, Zr and Ba, almost all of them require sampling of the archaeological objects, which is impermissible in many cases.

According to our present knowledge (Biró 2014), there exist three main types of Carpathian obsidian. The oldest (15–16 million years) black or transparent greyish Carpathian 1 (C1) is the best quality, it appears around Viničky, Mala Bara, Kašov and Cejkov in Slovakia. The younger (10–12 million years) non-transparent black or grey, very rarely reddish-brown Carpathian 2 (C2) comprises two subgroups, C2E from Mád–Erdőbénye–Olaszliszka and C2T from Tolcsva–Erdőbénye–Abaujszántó. They are from the Southern slopes of the Tokaj Mountains in Hungary. Finally, a third one, the Carpathian 3 (C3) has been discovered around Rokosovo, close to the western border of Ukraine. The best quality C1 has been transported for hundreds of kilometres, C2 has been circulated in long distance trade, while C3 being of lower quality has served only as local raw material—as was proved with the help of analytical results.

In the beginning of 2000s, the Hungarian National Museum launched a co-operation with the Budapest PGAA laboratory at the Centre for Energy Research (former Institute of Isotopes), Hungarian Academy of Sciences. We aimed to investigate whether the geochemical components measurable with PGAA (namely

the major elements of H, Na, Al, Si, K, Ti, Mn, Fe and the trace elements of B, Cl, Nd, Sm, Gd) are suitable to separate obsidian from other similarly appearing material like black opalites and other siliceous rocks, and if we would be able to differentiate between raw materials from various geological locations.

Already after the first set of measurements, it turned out that PGAA can easily discriminate between obsidian and other silicates (e.g. slags or silex). Also, it seemed to give a chance to identify various outcrops according to the compositions of obsidians from there (Kasztovszky et al. 2008). We have continued with systematic study of obsidian reference objects available in the comparative raw material collection (Lithotheca) of the Hungarian National Museum, as well as in the Prehistoric and Palaeolithic Collections of the Museum. Besides the existing reference materials in the Lithotheca collection, we have obtained comparative material by means of further fieldworks and also by scientific exchanges with several countries. Up to now, after more than 10 years, we have analysed around 180 archaeological artefacts and 160 geological reference samples. In our work, we focused on the research of the Carpathian region. Therefore, thanks to the international co-operations with many archaeologists and geologists, we have analysed archaeological objects from Hungary, Romania, Serbia, Croatia, Bosnia-Herzegovina and even from Poland. Geological references represent the most important Central European and Mediterranean sources, such as Tokaj Mts., Sardinia, Lipari, Melos, Antiparos, Pantelleria, Palmarola, Yali, Armenia and Anatolia.

As is known from the literature (Oddone et al. 1999; Tykot 1997), Instrumental Neutron Activation Analysis (INAA), X-ray Fluorescence Analysis (XRF) or Inductively Coupled Plasma Mass Spectrometry (ICP-MS) are quite sensitive and suitable to identify a series of trace elements in obsidians. Compared to the above methods, PGAA can detect fewer trace elements but it has some significant advantages. Since neutrons can go deep into the sample's material, the obtained compositional data are characteristic for the 'bulk' and are not affected much by surface contamination or weathering. Furthermore, it is not necessary to take a sample from a larger archaeological object, the whole object can be placed in the external neutron beam and a selected region can be investigated. Because of the relatively low beam intensity (10^7–10^9 cm^{-2} s^{-1}), the induced radioactivity is negligible and quickly decays. No damage of the objects has been ever observed.

Based on our PGAA measurements, we have found that boron (B) and chlorine (Cl) seem to be the elements that can most effectively discriminate between obsidians of different origin. For instance, boron concentrations are usually around some tens of ppm, but in case of Lipari obsidians, it can reach the order of 200 ppm, and at the same time, with high chlorine content. Besides B and Cl, iron (Fe), titanium (Ti) and alkaline elements (Na and K) were found also to be characteristic (Fig. 6.2). Usually, we construct bivariate or trivariate diagrams, or we apply statistical methods (Principal Component Analysis or Factor Analysis) to reveal similarities or differences between the samples (Kasztovszky et al. 2008).

So far, we have found the most definitive results with PGAA, when we have done provenance study of archaeological obsidians from Croatia, Serbia and

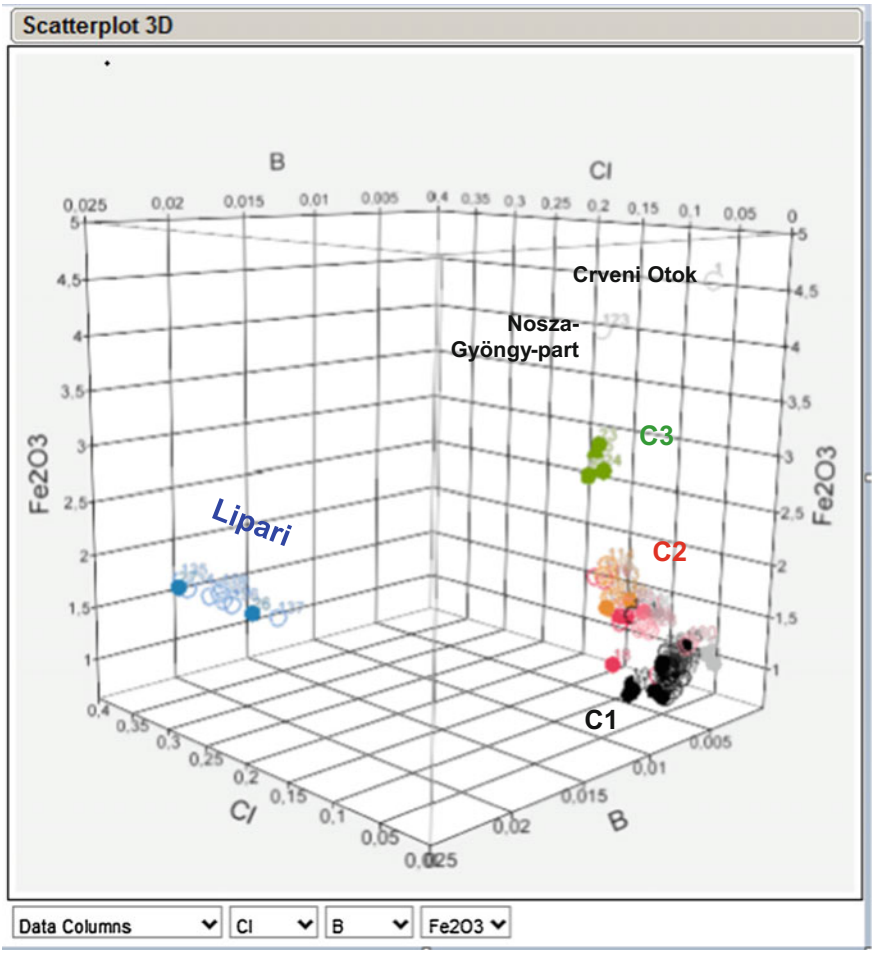

Fig. 6.2 Discrimination of archaeological and geological obsidians according to their elemental compositions measured with PGAA

Bosnia-Herzegovina (Kasztovszky et al. 2012). We have proved that there are two distinct types of archaeological pieces found in this territory. The ones from the Dalmatian shore turned out to be Lipari type, whereas the others found on the continental part proved to be Carpathian 1 (C1) type. In the case of the Dalmatian obsidian, other Mediterranean sources, such as Sardinia or Melos could be excluded with high confidence (Fig. 6.3). In another study, we have identified the furthermost occurrence of Carpathian 1 type obsidian in Upper Palaeolithic and Neolithic settlements found near Morsko, Rudna Wielka, Kowalewko and Cichmiana, Central Poland (Kabaciński et al. 2015)

Similarly to obsidian, we have also successfully applied PGAA to determine the provenance of Szeletian felsitic porphyry tools (Markó et al. 2003). Szeletian

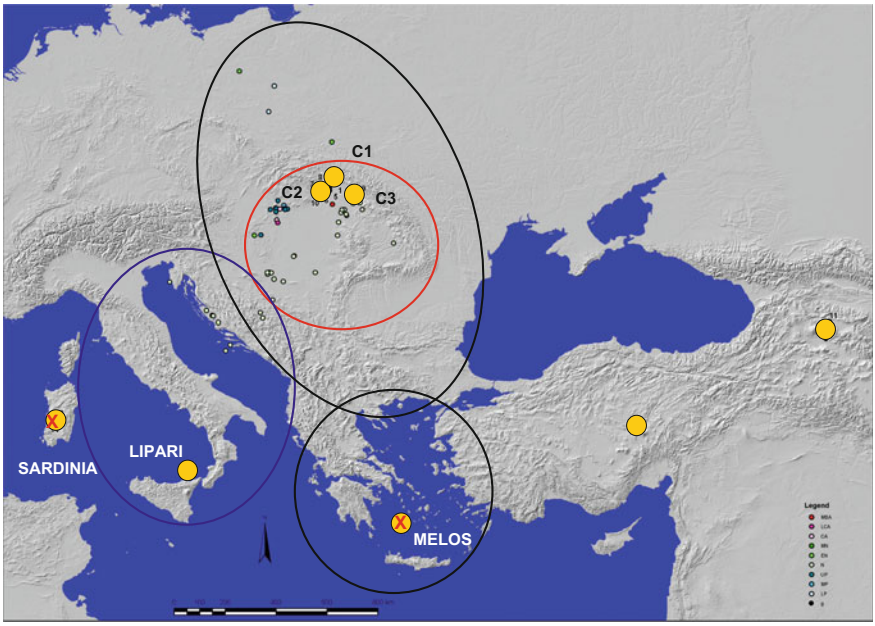

Fig. 6.3 Supposed raw material sources of archaeological obsidians found in the Central European (Carpathian) and Adriatic regions

felsitic porphyry was another popular prehistoric raw material; the name refers to the Szeleta cave in North-East Hungary where this specific raw material was first identified in archaeological context (Vértes and Tóth 1963). The first instrumental characterisation of this material was performed in the early 1960-ies (Vértes and Tóth 1963) by X-ray diffraction. In our studies (Markó et al. 2003), artefacts, macroscopically identified as Szeletian felsitic porphyry, turned out to be either Szeletian felsitic porphyry proper with relatively lower amount (75.3–82.4 wt%) of SiO_2, while for some siliceous rocks with similar appearance but different origin, the SiO_2 content was found to be between 95.5 and 98.5 wt%, which is characteristic for hornstone, radiolarite or for limnic quartzite (Fig. 6.4). Besides the silica content, concentrations of Na_2O, K_2O and TiO_2 were found to be discriminative factors. Partly on the basis of the analytical results, the intensive use of felsitic porphyry is well established in the Cserhát Mts. The on-site processing of the raw material in the Vanyarc type Middle Palaeolithic industry is documented at the distance of 100–125 km from the source area in the Bükk Mts.

Equally successful provenance research was performed on Neolithic polished stone objects made of greenschist-metabasite varieties (high-pressure metamorphite, nephrite, serpentinite, greenschist and blueschist). The aim of the study was again to map and characterise prehistoric resources, taking into consideration contemporary geographical and socio-economic relations in the Central European

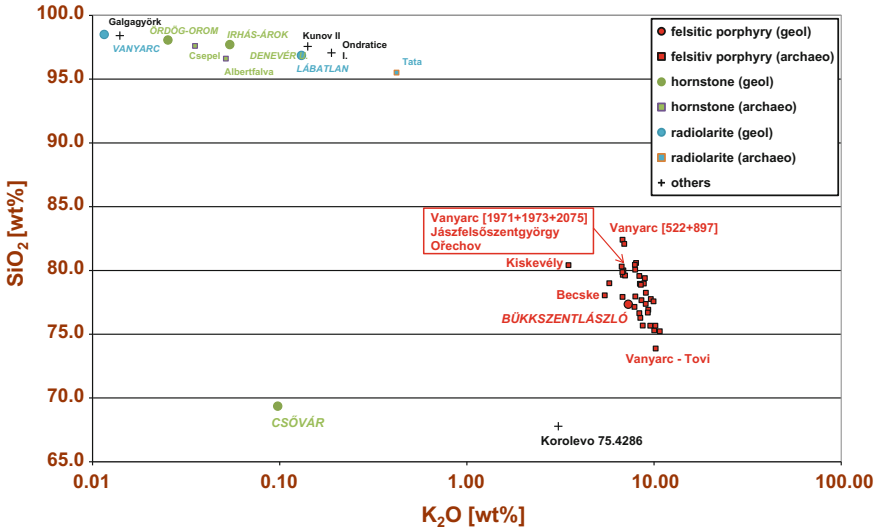

Fig. 6.4 Differentiation between Szeletian felsitic porphyry and silex samples, based on their Si- and K-contents

region, as well as "long distance" raw material sources known to play important role in the European prehistoric exchange network (Szakmány et al. 2011).

When we attempt to perform a provenance study of high silica-content siliceous raw materials, we will experience less success. Silex is a general term for very high silica-content (95–98 wt% SiO_2) sedimentary rocks, such as flint, radiolarite, chert, jasper or limnoquarzite. Unfortunately, because of the exceptionally high SiO_2 content, the possibility to detect other elements suitable for characterisation is very difficult for methodological reasons. It seems that we might have a chance to distinguish between silex types, but the identification of individual sources may require complementary (but not necessarily non-destructive) methods (Biró and Kasztovszky 2009).

6.3.2 *Lapis Lazuli—A Geological Gift*[2]

Archaeological finds, like beads, gems, seals and small decorative objects made of lapis lazuli are widely distributed in the ancient East and some date back as early as the second half of the fourth millennium B.C. in Central Asia. Also the blue pigment "ultramarine", used by the Grand Old Masters was nothing else but pulverised lapis lazuli. This paper provides a summary of multi-elemental characterization and

[2]Section written by Judit Zöldföldi and Zsolt Kasztovszky.

provenance analysis of lapis lazuli based on non-destructive Prompt Gamma Activation Analyses. The data show elemental distinctions between the well-known lapis lazuli sources, like Afghanistan, Russia, Chile and Ural Mountains. In the last few years, Prompt Gamma Activation Analysis, a non-destructive analytical technique has been applied in order to determine the place of origin of lapis lazuli. PGAA is one of the few non-destructive methods, which is applicable in bulk elemental analysis of valuable archaeological objects, like beads and cylinder seals. Some first successes in distinguishing lapis lazuli raw materials from different sources (Afghanistan, Lake Baikal, Ural, Canada and Chile) were already published (Zöldföldi and Kasztovszky 2003, 2009).

6.3.2.1 Lapis Lazuli as Archaeological Goods

Lapis lazuli, this opaque, deep blue gemstone looks back at a long history. Some of the most ancient lapis lazuli finds in Northern Mesopotamia are artefacts from Gavra XIII dated ca. 3500 B.C., and in Southern Mesopotamia—those from the Uruk II period (Derakhshani 1998). Among the most interesting Sumerian objects from precious minerals and gold in the Ur necropolis (26th c. B.C.) are the so called "Standard of Ur", with a mosaic inlay of small lapis lazuli and shell pieces, as well as goldbearing bull heads with lapis lazuli beard or standing goat figures with horns and decoration from lapis lazuli. Among some of the other objects in the British Museum in London can be noted rectangular and cylindrical seals, as well as a sceptre with triangular lapis lazuli inlay (Woolley 1934). Among the numerous poems from the period of the first civilizations in Mesopotamia, there exist an epic tale of Enmerkar and the Lord of Aratta (III mill. B.C.). It tells the story about the exchange of corn for lapis lazuli, gold and silver from the mountainous country Aratta needed for the building of palaces (Kramer 1952). Many researchers have been trying to trace the country Aratta, from where or through which the precious lapis lazuli and noble metals have been found or traded (Derakhshani 1998). According to some ideas, the country Aratta has to be located to the south or southeast of the Caspian Sea (Herrmann 1968), and according to others this country coincides in its location with the mountainous Badakhshan, because in the poem one can find expressions as "lapis lazuli in pieces", "they gather for her (goddess Innana) lapis lazuli from the deposits" or "lapis lazuli from the mountains" (Sarianidi 1971). Another hypothesis relates the Shahr-I-Sokhta site to the mythical country Aratta. Lapis lazuli has been included in epic poems of the Sumerians, which have also influenced later Babylonian or Hittitic versions of the myths: the Epic of Gilgamesh, the visit of the goddess Innana (she decorated herself with lapis lazuli jewellery) in the underground world; the myth for the origin of the mattock "with a forehead of lapis lazuli" and a lot of others (Kostov 2004).

From at least 4000 B.C. lapis lazuli was being traded. Royalty felt safer for the journey if they could placate the gods with gifts of sacred lapis lazuli; it was a kind of insurance. Never has lapis lazuli been quite as highly valued as it was intermittently over some two thousand years by the people of Sumer. Occupants of four

and a half thousand year old graves were determined to do all they could to placate the gods who ease the passage to the underworld (Searight 2010). Lapis lazuli, or za-gin of the Sumerians of the late third millennium B.C. Ur, was the great treasure (Moorey 1994), synonymous in literature with gleaming splendour, the attribute of gods and heroes. Thousands of lapis lazuli beads and objects have been found in graves excavated around huge temple complexes, as for instance at the greatest of Sumerian cities, Uruk, Ur and Mari or in the excavation of Qatna. The evocative name is a compound of "lapis", the Latin word for stone, and the Arabian word "azul", denoting the colour blue. It was one of the first stones ever to be used and worn for jewellery. Excavations in the antique cultural centres all around the Mediterranean provided archaeologists with finds which were left in tombs to accompany the deceased into the hereafter. Again and again this jewellery and objects crafted from lapis lazuli is the clear indication that thousands of years ago the people in Mesopotamia, Egypt, Persia, Greece and Rome cherished deep blue lapis lazuli. Especially in the oriental countries, it was considered as a gemstone with magical powers.

6.3.2.2 Mineralogy and Geology of Lapis Lazuli

Lapis lazuli is an opaque semi-precious stone consisting mainly of a blue mineral, lazurite, an alumo-silicate of the complex feldspathoid sodalite group, and can be described as an isomorphic combination of haüyn and sodalite (Webster 1975). The chemical formula for lazurite is $(Na,Ca)_4(AlSiO_4)_3(SO_4SCl)$, but with considerable variation in the amounts of SO_4, S and Cl (Hurlbut 1954). Additionally, pyrite and calcite together with relatively small amounts of accessory minerals are present in the stone lapis lazuli. The colour of lapis lazuli can vary from intense marine blue to violet blue, but lighter blue and green varieties also occur, depending on the shifting chemical composition. The finest and bluest lapis lazuli comes from just such pressures in the Hindu Kush mountain (Badakhshan) backbone of Afghanistan, but there are relatively few other occurrences of lapis lazuli worldwide: the Pamir Mountains in Tadjikistan, the Lake Baikal source in Siberia, Burma, Baffin Island in Canada, Edwards in N.Y. State (USA), the Green River Formation of Wyoming-Colorado-Utah, California (USA), Chile, Angola in Africa, Atlas Mountains in North Africa, Latium in Italy and the Ural Mountains in Russia. The sources of lapis lazuli are described by Rosen (1988) and Zöldföldi and Kasztovszky (2003) and are shown in Fig. 6.5.

Despite a number of studies, related to mineralogy and metamorphic conditions (Blaise and Cesbron 1966; Faryad 1999; Grew 1988), the origin of lapis lazuli and related mineralization remains unclear. Lapis lazuli is usually found in metamorphic limestone or dolomite, and typically in zones affected by contact metamorphosis (occurrence type 1). The basic chemical framework, thus, stems from igneous sources, as in other sodalite group minerals, but characterizing elements, such as calcium (Ca) and sulfur (S) lazurite have been picked up from the limestone/marble/dolomite surroundings. Lapis lazuli also characteristically contains calcite and pyrite

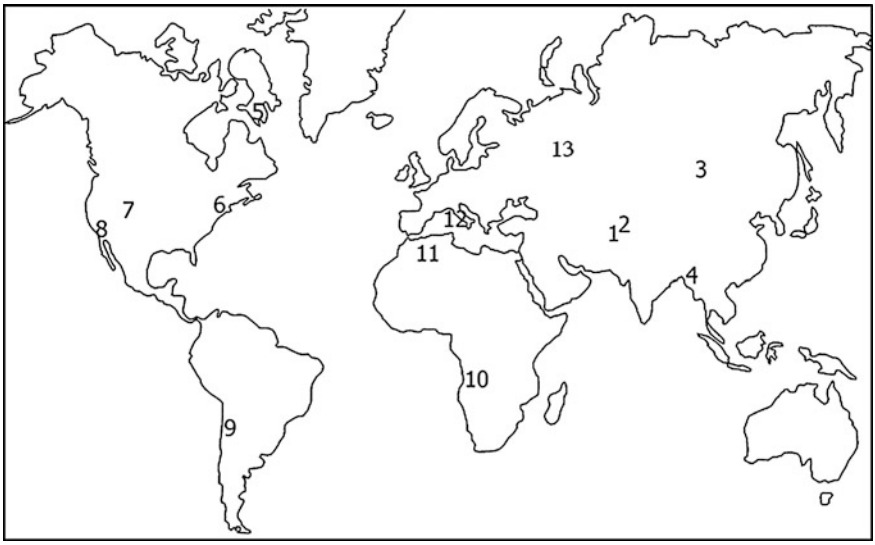

Fig. 6.5 Lapis lapis occurrences of the world. *1* Badakhshan, *2* Pamir, *3* Lake Bajkal, *4* Burma and Pakistan, *5* Baffin Island *6* Edwards, USA, *7* Wyoming-Colorado-Utah, USA, *8* California, USA, *9* Chile, *10* Angola, *11* Atlas Mountain, *12* Latium, Italy, *13* Ural

emanating from the limestone type host rock in addition to a number of minerals, which have igneous origins. According to Yurgenson and Sukharev (1984), the lapis lazuli deposits resulted from interaction between granite related hydrothermal fluids (Na-metasomatism) and marbles with high amounts of pyrite (occurrence type 2). A metamorphic origin for lapis lazuli deposits and whiteschists from primary evaporates and mudstone (occurrence type 3) was proposed by Kulke (1976), Hogarth and Griffin (1978) and Schreyer and Abraham (1976). The rather specific type of combination between a restricted range of igneous or evaporite rocks and carbonate (metamorphic) sediments, accounts for the rare occurrence of lapis lazuli.

Until recent years, it was supposed that the first lapis lazuli finds found at 4th millennia sites in Mesopotamia, Iran and the Indus came from the famous Badakhshan mines (Afghanistan). However, there is evidence as early as ca. 2700 B.C. for use of lapis lazuli from Lake Baikal and this source cannot be excluded simply because of its long distance from Mesopotamia (Buchanan 1966). Moreover, there is evidence that lapis lazuli from 3rd millennium Shahr-I-Sokhta originates from the Pamir Mountains in Tadjikistan, the Chagai Hills in Pakistan and from Badakhshan in Afghanistan, thus destroying the generally accepted hypothesis of only one supply source (Casanova 1992; Delmas and Casanova 1990).

Until recent times, it was not possible to differentiate between the lapis lazuli from Afghanistan and other sources by any mineralogical and chemical examination. Herrmann reports that different scientific tests failed to distinguish Afghan from Baikal lapis lazuli (Herrmann 1968). There used to be few scientific methods

available, including mineralogical investigation, trace elements analyses by X-ray fluorescence and optical spectroscopy (Herrmann 1968), as well as atomic absorption spectroscopy (Chakrabarti 1978; Faryad 2002; Herrmann 1968; Hogarth and Griffin 1978; Casanova 1992). There are differences in the percentages of MgO and K_2O in lapis from Afghanistan, Russia, Italy, the Pamirs, Baikal and Burma (Hogarth and Griffin 1978). Unfortunately, all the above investigations are definitely destructive. As lapis lazuli is a very rare and precious archaeological material, in most cases they are not allowed to undergo destructive analytical investigations. Lo Giudice et al. (2009) and his co-workers described differences in the cathodoluminescence and ionoluminescence behaviour of different lapis lazuli raw materials. Re et al. (2011) reported about the micro-PIXE characterization of lapis lazuli. They turn their attention to single phases and investigations of the surface instead of the whole rock; in particular on two main minerals, the lazurite and diopside.

6.3.2.3 Experimental Setup

From 2002, we have tried to explore how effectively we can apply the bulk elemental composition—measured by PGAA at the Budapest Neutron Centre—to determine the provenance of lapis lazuli. Bulk samples (whole rocks) have been irradiated by a horizontal cold neutron beam at the Budapest Research Reactor. The thermal equivalent intensity of the beam was 10^8 cm^{-2} s^{-1}. The upgraded PGAA facility is described by (Szentmiklósi et al. 2010). The acquisition time was chosen between 2200 s and 50,600 s, in order to detect as many trace elements as possible. The prompt-gamma spectra were detected by a calibrated Compton-suppressed HPGe detector, the spectra were evaluated using the Hypermet-PC program (Molnár et al. 2002; Révay et al. 2005). The basis of the quantitative analysis was the standardisation using k_0-method, a kind of comparator method, which was earlier used in INAA, and later adopted in PGAA (Molnár et al. 1998; Révay 2009). The applied PGAA spectroscopic data libraries were developed at the Institute of Isotopes (Révay et al. 2001a, b). The effect of the spectroscopic background originating from the surrounding material, was taken into account, based on accurate background measurement.

Reliability of the PGAA method was checked several times on geological standard reference materials. With PGAA, we were able to quantify all the major components and some trace elements in whole rock samples. Concentrations of detectable chemical elements are calculated in wt% or in ppm. As a convention in geochemistry, major components are given in oxide forms, calculated according to the oxidation numbers. The accuracy of the chemical analysis is mainly determined by the peak areas as they used in the efficiency calculation, in determination of partial cross-sections, as well as in analysis of unknown samples (Révay 2006). As a result, for major components, the typical relative uncertainties of concentrations are between 1 and 3 %. Since lapis lazuli is an inhomogeneous rock, the variation of composition within one piece of rock was tested on various cuts of the same rock.

Because of the relatively low intensity of neutron beam, the induced radioactivity is practically negligible and decays quickly. The biggest advantage of PGAA is the applicability to investigate whole archaeological objects or pieces of rocks without any sampling or destruction of the objects. Since neutrons can penetrate many centimetres deep into the sample material, one can obtain an average composition of a few cm^3 sample volume.

In comparison to the methods of contemporary researchers—Lo Giudice et al. (2009) and his co-workers who described differences in the cathodoluminescence and ionoluminescence behaviour of different lapis lazuli raw materials and Re et al. (2011) who reported about the micro-PIXE characterisation of lapis lazuli—we turn our attention to the non-destructive investigation of the chemical composition of the whole rock and not only the surface, which partially undergoes significant weathering due to time. For this purpose, in the last decade, Prompt Gamma Activation Analysis (PGAA) has been applied in order to determine the origin of lapis lazuli. PGAA is one of the few non-destructive methods which is applicable in bulk elemental analysis of valuable archaeological objects, like beads and cylinder seals. Some early successes were achieved in distinguishing lapis lazuli raw materials from different occurrences (Afghanistan, Pakistan, Tadjikistan, Lake Baikal, Ural, Canada and Chile).

6.3.2.4 Results and Discussion Related to Investigation of Lapis Lazuli

With PGAA we were able to detect the major components H, Na, Ca, Al, Si, S, Cl, K, and the accessory elements Mg, Fe and Mn. In addition, the trace elements of B, Sc, V, Cr, Co, Sm and Gd were also identified.

The geological history and mineral compositions described above imply the presence of fluid phases with high concentrations of CO_2, halogens and S during metamorphism of the rocks. S and halogens (e.g., Cl, B) are incorporated in the following minerals: Cl and B in scapolite, sodalite, biotite, amphibole and apatite; S in haüyne, lazurite, scapolite, pyrite and pyrrhotite and F in apatite, biotite, amphibole, titanite and clinohumite. With the exception of accessory pyrrhotite, pentlandite and some scapolites, S-bearing minerals originated during retrogression and metasomatism.

Based on this geological and mineralogical knowledge, we have chosen the elements S, B and Cl to distinguish the lapis lazuli samples from different occurrences. Unfortunately, the detection of F is impossible with the PGAA method, because of the very low neutron capture cross section of fluorin.

With the help of PGAA all the major (Si, Al, Ti, Fe Mn, Mg, Ca, Na, K, S, H, occasionally P, C) and some accessory elements (Cl, B, Sm, Gd, in some cases Nd, V, Co, Sc) of lapis lazuli were possible to quantify. As an average chemical characteristic of bulk lapis lazuli samples, the less variable major element concentrations are the following: 40–45 wt% SiO_2, 9–11 wt% Al_2O_3, 0.02–0.05 wt% MnO, 10–13 wt% MgO, 14–21 wt% CaO, 4–6 wt% Na_2O, 0.4–2.0 wt% K_2O and 0.6–1.2 wt% H_2O. Although, the calcium content showed larger variation, it cannot

be considered as a characterizing element of certain rock sources, since it is directly correlates with the calcite content. Applying discrimination calculations with concentrations and concentration ratios, the PGAA analyses proved that based on the bulk chemical composition, the lapis lazuli from Chile and Ural can be clearly distinguished from each other and from the Afghan and Baikal sources. However, the raw material' compositions of Afghanistan and the Baikal region significantly overlap (Fig. 6.6). We have found the most important discriminative elements to be Cl, S, Fe and B. Especially, Cl, B and S are basic variable components of lazurite, the major blue mineral phase. From this data, these elements are assumed to behave sensitively in different (contact metamorphic or Na-metasomatic) conditions of the petrogenesis. However, iron and sulphur are the major constituents of one of the important impurities of the lapis lazuli, the pyrite (FeS_2). To eliminate the chemical effect of pyrite, normalization by SO_3/Fe_2O_3 ratios was applied for the bulk chemical data (Fig. 6.7). The Chilean lapis source is characterized with the highest

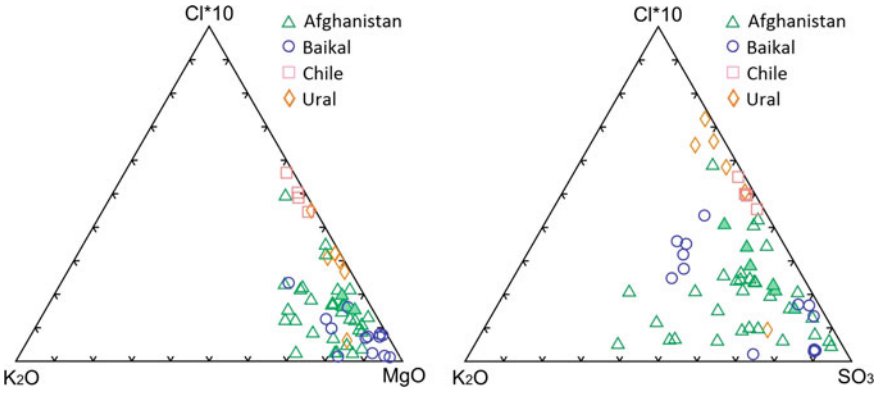

Fig. 6.6 Ternary plots showing the variable major element concentrations

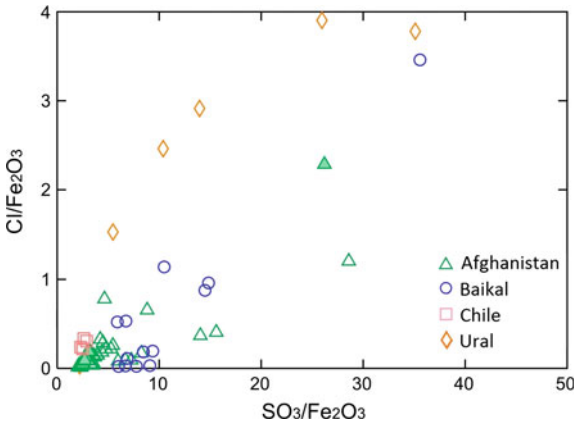

Fig. 6.7 Sulphur and chlorine contents of lapis lazuli samples, normalized by iron content

chlorine, iron and sulphur content. The lapis lazuli of the Ural source has medium chlorine concentrations, while the Fe, S and also the B content is much lower than that of the Chilean. The lapis lazuli samples from the Afghanistan localities show the widest scattering in their chemical composition.

The most significant chemical characteristics of these samples are the highest boron content and the medium Fe, S, and Cl concentrations. As a methodological aspect, one sample from Afghanistan and another from Baikal Lake was selected for the investigation of their heterogeneity. For this reason, two pieces of lapis lazuli blocks (Afghanistan and Lake Baikal) have been cut into 4 slabs and measured separately (Fig. 6.8). Figure 6.9 shows that the element ratios of Cl/SiO_2 and B/SiO_2 are not affected by the sample heterogeneity, and allow the distinguishing between the different occurrences, with minor overlaps.

In its present state, a preliminary database of chemical composition of lapis lazuli raw materials from the main known sources is appropriate to distinguish between the most relevant quarries.

In addition to the above mentioned calculations, Principal Component Analysis —a multivariate statistical method—has been carried out to seek patterns of differential distribution of the samples within the compositional space. This would

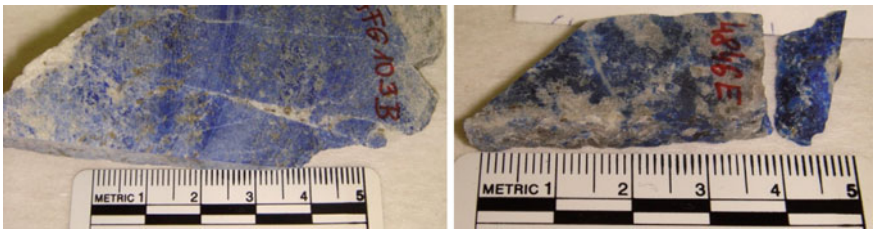

Fig. 6.8 Slabs of the lapis lazuli samples from Afghanistan and Lake Baikal

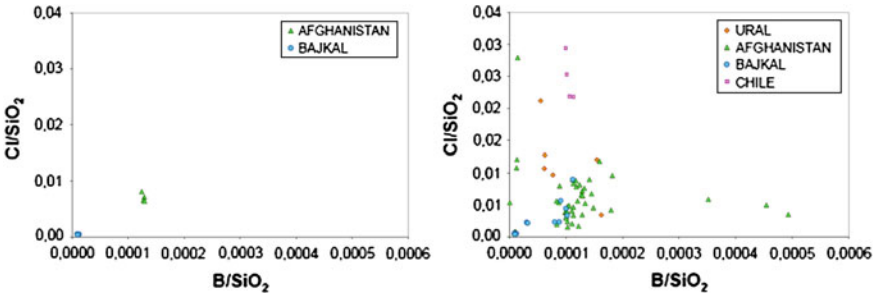

Fig. 6.9 Cl/SiO_2 and B/SiO_2 ratios; *left* measurements of the same block but in different slabs; *right* discrimination diagram of the raw materials stems from well-known lapis lazuli occurrences

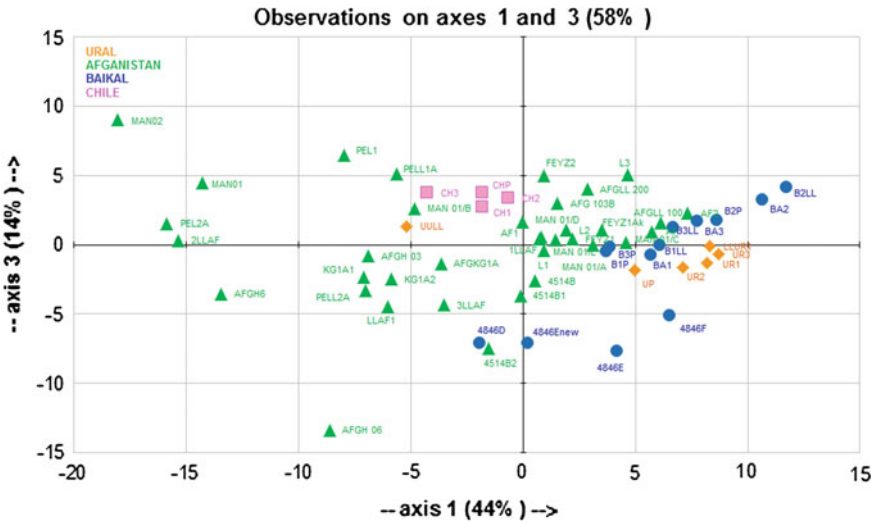

Fig. 6.10 Principal Component Analysis (PCA) analyses, including all the analytical data of lapis lazuli raw material

allow us to see the data dispersion when the correlation among the elements was part of the data analysis. As the components are linear combination of all the original composition data, PCA can reveal some significant differences/similarities between the objects—even in the absence of rigorously defined groups. Figure 6.10 shows the 1st and 3rd Principal Components, calculated from all the analytical data of lapis lazuli raw material that allows obtaining different clusters on the basis of the provenance of natural lapis lazuli deposits. This approach, tested on a large number of samples, shows that a significant discrimination of lapis lazuli coming from different natural deposits is possible based on the bulk chemistry, although some overlaps occur. This knowledge could be of great relevance in the identification of the provenance of lapis lazuli in archaeology and works of art and in the discrimination between their natural or synthetic origin.

6.3.2.5 Concluding Remarks

Lapis lazuli is a very rare and precious archaeological material, which in most cases is not allowed to undergo destructive analytical investigations.

PGAA is one of the few non-destructive and methods which is applicable in elemental analysis of these valuable archaeological objects. With the help of PGAA we were able to measure all the major and accessory components of lapis lazuli. Cl/SiO_2 and B/SiO_2 are not affected by the sample heterogeneity, and allow the distinguishing between the different sources, with minor overlaps.

6.3.3 *Stone Travellers. Contribution of Non-invasive Nuclear Techniques to Determine Culture Identity, Mobility and Interaction in the Recent Prehistory of South Portugal*[3]

6.3.3.1 How to Understand the Perdigões Interaction Network

Studies of provenance are a valuable tool for archaeological research, especially when dealing with the socio-economic and cultural impact of trade routes.

The Perdigões site is one of the largest known Portuguese Chalcolithic ditched enclosures, occupied during the late 4th–3rd millennium B.C. (Valera et al. 2014a) in the Reguengos de Monsaraz region, in the South of Portugal.

This circular shaped site spreads over an area of about 20 ha, and presents twelve roughly concentric ditches (Márquez et al. 2011). Several interdisciplinary teams have been working at this site. Work developed so far suggests the existence of a very complex range of activities, namely burial ground areas (Lago et al. 1998; Valera et al. 2000, 2008, 2014b). The burial remains are diversified and mainly consist of pottery, lithic artefacts, stone (marble, limestone and others) and bone and ivory idols, pecten shells, ivory combs, adornment artefacts, etc. (Valera 2008, 2012a, b).

Pottery artefacts include all the typical morphologies of the Late Neolithic and Chalcolithic of the South West of the Iberian Peninsula and there are differences between the style, production technology and provenance of funerary and domestic pottery (Dias et al. 2005).

At the Perdigões ditched enclosures several funerary contexts have been excavated dating from the Chalcolithic (3rd Millennium B.C.). In the eastern side there is a tholoi tomb necropolis and in the centre some funerary pits with the deposition of cremated human remains. Excavations reveal that the funerary practices in these two areas of the enclosure present different ritual procedures, not just in terms of architecture and body manipulation, but also in terms of what kind of votive materials were use (they differ in category and typology).

One of the item types found in the necropolis is stone idols, but with different typologies and raw material, apparently mostly made of marble or limestone, suggesting different origins for these artefacts, since both rocks do not occur locally, but regionally. Some questions remain to be answered, like their compositional nature and their provenance.

Stone idols in Chalcolithic were found in several archaeological sites from Estremadura and Southern Portugal. But, so far, no archaeometric approach has been made to these materials. This compositional study will be the first one to be performed, especially aiming to contribute to provenance issues, by means of

[3]Section written by M. Isabel Dias and António Valera.

compositional studies of both artefacts and potential raw materials, and to the characterization of the diverse funerary contexts, by answering questions such as:

(1) Is it possible to differentiate raw materials used in the stone idols of the two types of funerary contexts—tholoi tomb necropolis and funerary pits? It is important to extend the evidence that these two areas of the enclosure have diverse funerary practices, with evidences of different ritual procedures, architecture, body manipulation and votive materials.
(2) Provenance/circulation issues: do these stone idols point to different provenances, with diversified raw materials (local? regional? unknown?) like the more differentiated provenances already found for ceramic from funerary contexts as opposed to non-funerary pottery (Dias et al. 2005)?

So, one of the main goals of this work was to determine if diverse raw material resources were used by studying the composition of a set of stone idols and ritual stone vessels, together with geological samples (marbles and limestones), trying to evaluate the degree of compositional homogeneity between idols, as well as possible areas of origin, all contributing to understanding the interaction network in which Perdigões was involved. Another important goal of the study was to determine whether Prompt Gamma Activation Analyses could be successfully used to trace the source(s) of those Chalcolithic artefacts made of carbonate rich raw materials.

Scientific data on the provenance of the ornamental stone material of individual monuments and archaeological objects, like sculpture, are becoming increasingly available. For the Iberian Peninsula, many studies have dealt with the distribution and (archaeological, petrographic and geochemical) characterisation of the ornamental stones especially for Roman chronologies, considering the main Roman exploitation centres (white and coloured marbles), such as the white marbles of Estremoz, Almadén de la Plata, Macael and Sierra de Mijas, and the coloured stones of Antequera, Sintra, Broccatello, Buixcaró, Santa Tecla and Espejon (i.e. Lapuente 1995; Lapuente and Turi 1995; Morbidelli et al. 2007; Domínguez Bella 2009; Origlia et al. 2011; Beltrán et al. 2012; Mañas Romero 2012; Taelman et al. 2013; Taelman 2014).

A large problem in sourcing carbonate rich artefacts is that macroscopically they may look similar, even if they come from different sources. From a mineralogical point of view, they are almost pure $CaCO_3$ with a very heterogeneous mixture of impurities. As already noticed for sourcing microcrystalline quartz artefacts (Crandell 2012), also in this case of carbonate artefacts, especially those deriving from the metamorphic evolution of previous carbonates (marbles), the stone materials are often rather similar to each other in many respects (i.e. mineralogical, physical–structural and chemical), and their sources are thus difficult to identify. Due to the fact that impurities are generally heterogeneous in this kind of geological source, a significant overlap with other sources may occur.

Among the most common impurities, such as silica, alumina, iron and manganese oxides, carbonates, carbonaceous materials, the alkalies occur usually in very small

amounts in limestones and marbles. Impurities present in the limestone during recrystallization affect the mineral/chemical composition of the marble that forms, thus the difficulty in source differencing of this kind of materials.

Another important issue related to the analysis of these artefacts is the fact that the objects involved are often unique in nature. To achieve the main goals, and regarding the rareness and importance of these stone artefacts only non-invasive analysis is possible. Analysing objects of historic and archaeological nature such as the stone idols should be non-destructive, i.e., respecting the physical integrity of the material object, but must be sensitive, so that provenance analysis can be done by means of not only major elements but also trace-element fingerprints, and multi-elemental, so that in a single measurement, information on many elements is obtained simultaneously. Also, to better obtain provenance correspondence between artefacts and potential raw materials, the same methodological approach should be performed on both.

Prompt Gamma Activation Analysis is one of the new techniques available to deal with this problem. Its basis is the radioactive capture of neutrons, or the (n,γ) reaction. During this nuclear reaction, an atomic nucleus captures a thermal or sub-thermal neutron, and emits a number of gamma photons promptly (Révay and Belgya 2004). Because of the low intensity of external neutron beams, PGAA can be considered non-destructive, and is applicable to objects that must be preserved intact and do not require sample preparation, being positioned directly in the neutron beam. Indeed, in most cases no significant long-lived radioisotopes are produced during the analysis. After some days of cooling, the analysed artefacts are in perfect condition to be returned to museums, collectors, and researchers. Nevertheless it is important to emphasize that PGAA, due to the high penetrability of the neutron will give the composition of the bulk material (not possible to evaluate composition of the body separately from the surface of the objects). This nuclear analytical technique for non-destructive quantitative determination of elemental compositions has been successfully applied to characterize archaeological objects made of various rocks (Kasztovszky et al. 2008). In the case study of this work the PGAA facility used was the Budapest Research Reactor, which has become a leading laboratory for applications of PGAA in archaeometry (Szilágyi et al. 2012; Kasztovszky et al. 2004).

6.3.3.2 Stone Idols and Ritual Stone Vessels Versus Geological Materials

Limestones in Portugal occur mainly near the shore, to the north of Lisbon and in the Algarve region, in the south. The main mining district of ornamental limestones is the Maciço Calcário Estremenho (MCE), located 150 km north of Lisbon. It is a limestone massif from the Mesozoic carbonated rocks tectonically elevated. Most of the MCE limestones are fine to coarse-grained calciclastic sparitic rocks. The region of Pêro Pinheiro, just North of Lisbon, is also one of the most traditional production centres of ornamental stones of Portugal. Quarrying has signs that it has been

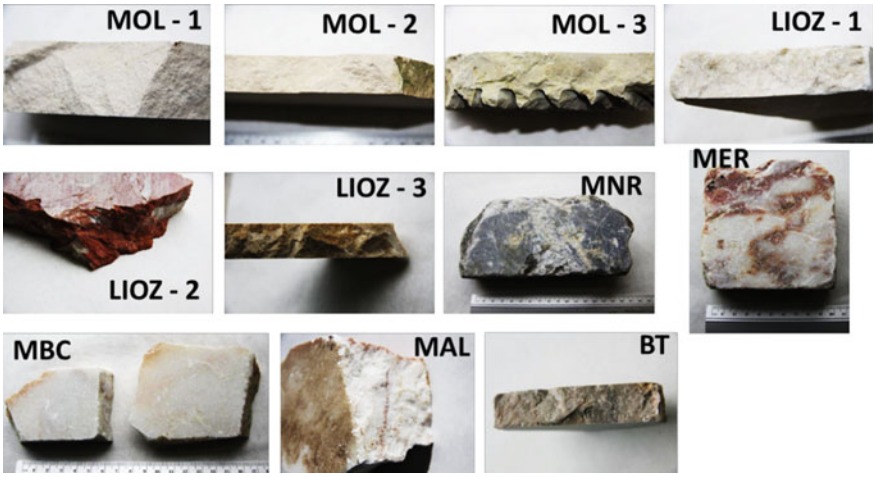

Fig. 6.11 Photos of the samples described in Table 6.1

started in Roman times. In the Algarve region ornamental stones are extracted near the localities of Escarpão (municipality of Albufeira), Mesquita (municipality of S. Brás de Alportel) and Santo Estevão (municipality of Tavira).

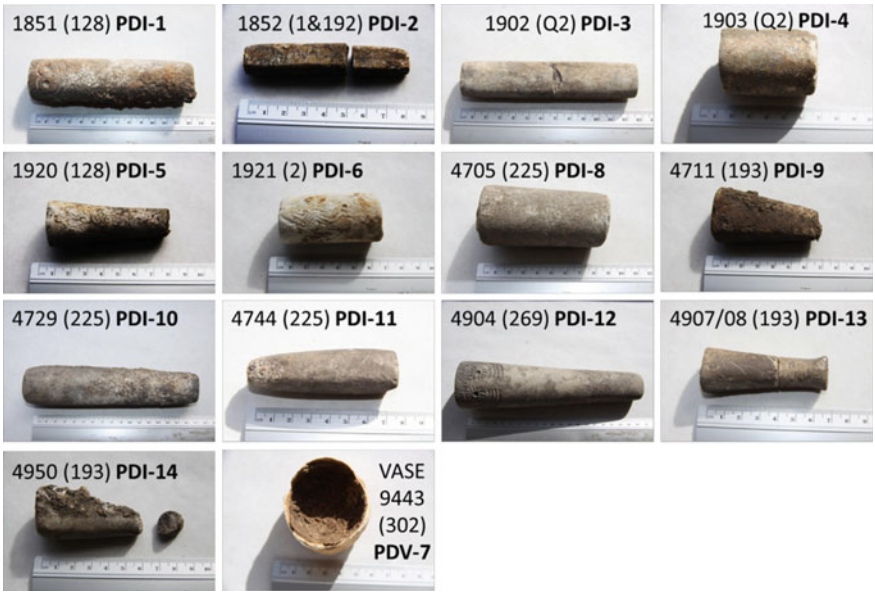

Fig. 6.12 Stone artifacts from Perdigões archaeological site; Inventory (UE) **Ref. Lab**

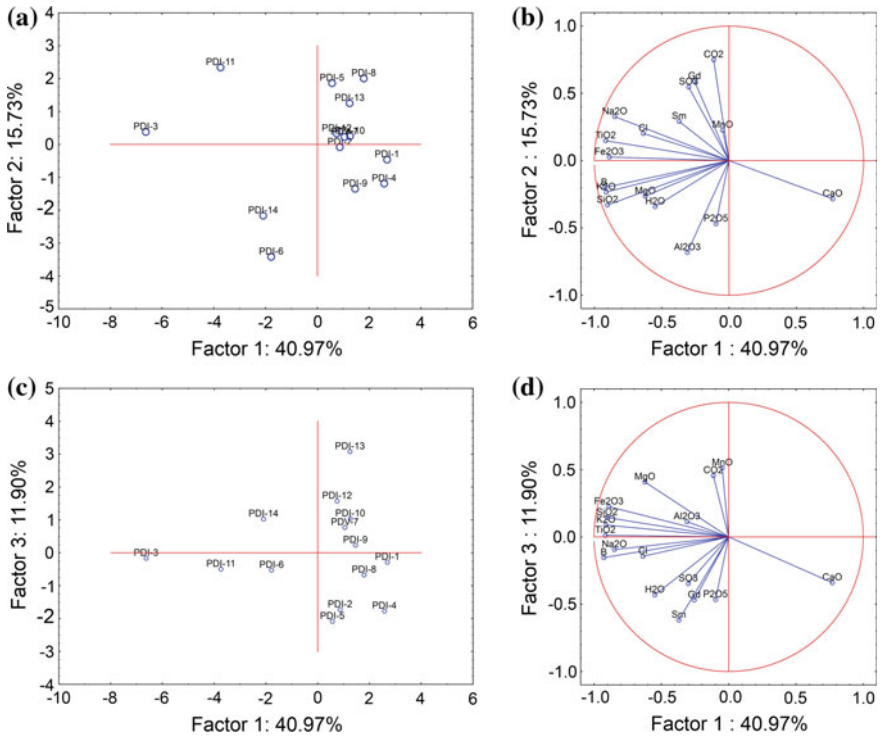

Fig. 6.13 Projection of the cases (**a**) and of the chemical elements (**b**) as variables, on the factor-plane 1 × 2, for artefacts; Projection of the cases (**c**) and of the chemical elements (**d**) as variables, on the factor-plane 1 × 3, for artefacts

Marbles occur mainly in the Alentejo region, where the Anticlinal de Estremoz is the main production centre. The earliest evidence for exploitation of this resource in this region dates back to the year of 370 B.C. (Martins and Lopes 2011). They present a large spectrum of colours, from white to dark grey, but the most common are the light-cream coloured with streaks of different tonalities (Figs. 6.11 and 6.12).

Based on archaeological and geological considerations, in the investigations for possible geological sources of stone idol artefacts found at Perdigões, the sources were separated into three categories: (a) nearby sources (∼40 km distance—area known as the "marble triangle" Estremoz—Borba—Vila Viçosa, in Alentejo's northeast, between Sousel and Alandroal, contains Portugal's most important ornamental rock deposit.), (b) moderate distance areas (∼130 km—limestone from Tavira—Tavira Breccia) and (c) remote areas (160–200 km—Limestones from Pêro Pinheiro—Lioz and from the Maciço Calcário Estremenho—Moleanos) (Table 6.1; Fig. 6.13).

Seven limestone samples (Moleanos limestone: MOL-1, MOL-2, MOL-3; Lioz limestone: LIOZ-1, LIOZ-2, LIOZ-3; Tavira breccia BT) and four marble samples (MNR, MAL, MBC, MER) were analyzed. Regarding artifact samples, thirteen stone idols and one votive vase were analyzed (Fig. 6.12).

For both artifacts and geological materials, the same methodological approach was used, so by using the same variables better comparisons and provenances ascriptions of provenance are achieved.

Prompt Gamma Activation Analysis of a total of 14 artefacts and 11 geological samples has been performed at the PGAA instrument of the Budapest Research Reactor. The PGAA instrument operates on a 7.6×10^7 cm^{-2} s^{-1} intensity guided horizontal cold neutron beam. The samples have been irradiated with a beam collimated to 24 mm^2 or 44 mm^2. The prompt- and delayed gamma photons emitted after neutron capture were detected with an HPGe detector in Compton-suppression mode. The typical acquisition time varied between 2300 and 8300 s, in order to collect statistically significant counts. The collected spectra have been evaluated with the Hypermet PC software; the element identification and calculation of concentrations are based on BNC PGAA library.

Table 6.1 Geological materials

Sample reference	Sample description	Note
MOL-1	Limestone "Moleanos"	Moleanos—Aljubarrota, Alcobaça (board of the Natural Park of Serra D´Aires and Candeeiros). Leiria. Central Portugal (~100 km North Lisbon)
MOL-2	Limestone "Moleanos"	Pé da Pedreira—Alcanede (Natural Park of Serra D´Aires and Candeeiros), Santarém, Portugal.
MOL-3	Limestone "Moleanos"	Ataija, Aljubarrota, Alcobaça. Leiria
LIOZ-1	Limestone "Lioz"	Pero Pinheiro, Sintra.
LIOZ-2	Limestone "Lioz"	Fervença, Terrugem, Sintra
LIOZ-3	Limestone Lioz—Lioz de Montemor	Montemor, Sta Maria de Loures, Loures, Lisboa
MNR	Marble "Negro Ruivina"	Lagar, Vila Viçosa Santos, Bencatel, Vila Viçosa, Évora
MER	Marble "Estremoz Rosado"	Estremoz (Santa Maria) Évora, Primavera, Bencatel, Santos, Vila Viçosa
MBC	Marble "Borba" "Estremoz" corrente	Évora, Estremoz/Borba/Vila Viçosa
MAL	Marble Alandroal	Alandroal
BT	Limestones—Brecha "Tavira"	Julião, Sta Catarina do Bispo, Tavira, Faro, S. Brás de Alportel

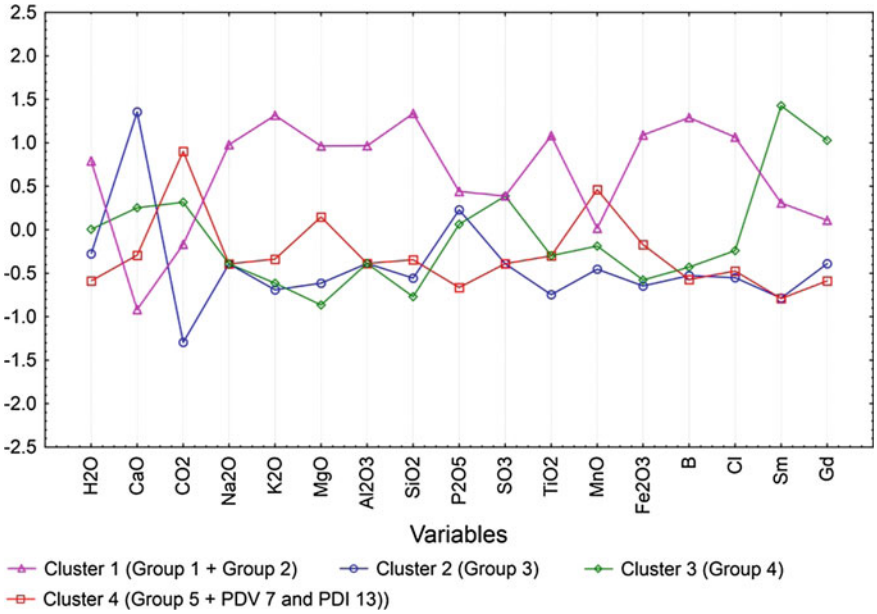

Fig. 6.14 Plot of means for each cluster by using the k-means clustering method on chemical contents as variables and artefacts as cases

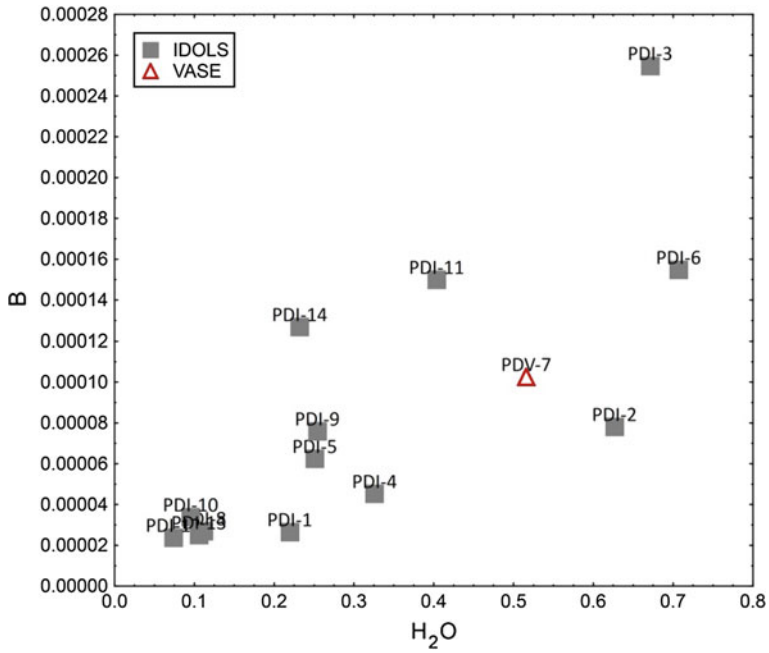

Fig. 6.15 Scatterplot of B against H_2O of Perdigões stone artefacts

6.3.3.3 Tracing Stone Artefacts at Perdigões Site

The first non-destructive analytical approach using PGAA for studying the limestone and marble artefacts from Perdigões, together with potential raw materials, provided chemical data that can be used to differentiate, from a compositional point of view, both artefacts and geological sources.

For the statistical interpretation of the PGAA data, only the oxides/elements which were above the quantification limit in most of the samples were used i.e. CaO, CO_2, LOI (H_2O), SiO_2, $Fe_2O_3^t$, MnO, K_2O, MgO, TiO_2, B, Cl, Sm and Gd.

The materials used to make the idol stone artefacts at Perdigões do not vary widely in the visual characteristics, as well as in their typology. The most commonly used materials appear to be limestones and/or marbles.

CaO and MgO are the most important elemental oxides in carbonates. In calcitic marble CaO is usually in the order 50–54 wt% while MgO is <15 wt%. Dolomitic or magnesian type marble has CaO values in the range of 28–31 % and MgO values in the range of 15–21 wt% (Goldschmidth et al. 1955).

In the studied samples CaO is the prevailing major component, ranging from 50 to 57 wt% in artefact samples, and between ~51 and ~56 wt% in the geological samples. All analysed samples have a relatively low MgO concentration (<2 wt%). The MgO content in the marble samples range from 0.4 to 0.61 wt%, in the limestones ranges from 0.26 to 1.6 wt%, and in the stone idols from 0.21 to 0.80 wt%. In Lioz-2 limestone no Mg was detected, and in 4 idols (PDI 1, 2, 4 and 8) and in the vase (PDV 7) also no Mg was detected.

The distribution of Ca/Mg and its reciprocal Mg/Ca ratio in limestones were utilized by Todd (1966) as a parameter for chemical classification (Table 6.2). The studied geological samples are all included in calcitic type marble and pure limestone, but the breccia Tavira sample (BT) is a limestone more enriched in Mg. Regarding the artefact samples, they are all pure limestones/calcitic marbles.

Mg/Ca ratios in raw geological samples vary from 0.029 to 0.009 %, and in artefacts from 0.01 to 0.007 %. In order to establish the paleo-environment of deposition Marschner (1968) pointed out that the Ca/Mg ratio is indicative of stability condition during the formation of carbonate rocks and any decrease in Ca/Mg ratio is related to corresponding increase in salinity. The high value of Ca/Mg ratio indicates comparatively less evaporation of sea water during the time of limestone deposition. From the results we may infer that Lioz limestones have in general lower Mg/Ca ratios (Table 6.2).

Table 6.2 Chemical classification of Shella limestone[a]

Descriptive term	Standard ratio Ca/Mg	Reciprocal ratio Mg/Ca
Pure limestone	100.00–39.00	0.00–0.03
Magnesian limestone	39.00–12.30	0.03–0.08
Dolomitic limestone	12.30–1.41	0.08–0.71

[a]Todd (1966)

Silica in carbonate rocks is contributed mainly from silicate minerals. The SiO_2 content in the marble samples range from 0.64 to 3.7 %, in the limestones ranges from 0.27 to 2 %, and in the stone idols from 0.09 to 2.9 %.

The alkali elements such as Na and K may be indicative of salinity levels (Na and K concentration in marbles tend to decrease with increase in salinity). Sodium was below detection limit in almost all the samples (only in two idol samples it was detected). Potassium was not detected in most of the geological materials, only in the Lioz Limestones and Ruivina and Alandroal marbles, ranging from 0.031 to 0.101 %; in the idol samples potassium was detected in half of the samples, ranging from 0.010 to 0.138 %. The smaller but appreciable concentration of manganese in carbonates is probably also attributable to similarity in ionic size with ion Ca^{2+}. In marble samples manganese ranges from 0.0059 to 0.023 %, in limestones from 0.0074 to 0.0100 %, and in stone artefacts from 0.0035 to 0.0233 %. The low content of Mn in the studied samples may be attributed to the substitution of Mn by Ca.

The other oxide contents are generally low. Alumina was detected in a few samples, indicative of the absence of alumina-silicates, most of them the geological ones, ranging from 0.25 to 1.5 %. Iron oxide (Fe_2O_3 total in %) was detected in most of the samples, with a maximum of less than 0.39 %. In the marble samples iron ranges from 0.069 to 0.17 %, in the limestones from 0.068 to 0.19 % and in the stone artefacts from 0.05 to 0.39 %. Titanium oxides were also detected in most of the samples, in general with low values, ranging in the geological samples from 0.0066 to 0.025 % and in the stone artefacts from 0.0024 to 0.044 %. Phosphorous and sulphur were detected in very few samples, the first only in the idols (ranging from 0.016 to 1.9 %), and the second in a few idols and limestones with a maximum of less than 0.16 %.

We can infer loss on ignition (LOI) by the content of volatiles (CO_2, H_2O) present in the samples. In general, the sums of the two values are high, indicating high volatile content and by implication high carbonate content.

Regarding trace elements, immobile trace elements such as the Rare Earth Elements (REE) are usually important for provenance determination. With PGAA we have determined Sm and Gd. Gadolinium was detected only in two geological samples, and in a few stone artefacts, varying from 0.061 to 0.445 μg/g. Samarium contents in marbles ranges from 0.089 to 0.349 μg/g, in limestones from 0.041 to 0.380 μg/g, and in the stone artefacts from 0.038 to 0.446 μg/g. No Sm was detected in two idols and in the vase.

Boron contents of limestones are generally low, and are only elevated when the clay or organic contents are high, largely incorporated in illite, being used as a paleo-salinity indicator and marine environment. In the limestones studied in this work B contents were observed from 0.337 to 3.170 μg/g, and in the marble samples lower contents were detected, from 0.315 to 1.572 μg/g. In the artefacts B content also has a varied range, from 0.238 to 2.540 μg/g.

Chlorine was not detected in one marble sample and the other two have similar Cl contents (0.0023 to 0.0029 %). In two Lioz limestones Cl was not also detected, varying in the others from 0.0016 to 0.0079 %. Regarding artefacts, Cl was not detected in three, and in the others varies from 0.0011 to 0.0153 %.

It is important to emphasize that PGAA results correspond to the bulk sample, and idols have not been cleaned from surface deposits, which appears on some of them in considerable amounts, and is particularly enriched in crushed bones and soil. A special care was taken in order to evaluate whether the analysed chemical contents might have been affected due to bone contamination, and not specifically to the nature of the geological source, but no correlation was directly established between the analysed artefacts, and the chemical contents that are usually present in bones, and are also used for paleo nutrition research (Allmäe et al. 2012).

A statistical approach was performed for the fourteen stone idols analysed, as well as for the geological materials, taking into consideration chemical elements as variables. The analysis of obtained results for the stone idols, particularly the statistical results obtained by PCA and clustering methods applied on the chemical contents (Figs. 6.13 and 6.14), clearly detach the following groups: Group 1—PDI 3 and PDI 11; Group 2—PDI 6 and PDI 14; Group 3—PDI 1, PDI 4, PDI 9; Group 4—PDI 2, PDI 5, PDI 8; Group 5—PDI 10, PDI 12. Idol sample PDI 13 is not similar to any of the others. The vase sample analysed (PDV 7) has also a different chemical behaviour.

It is important to emphasize that the 2 samples from Group 1 were gathered in the cluster analysis mainly due to lower CaO contents and, because they are the only ones where Na was detected. Concerning the other elements significant differences were observed questioning the possibility of a same source, particularly PDI 3 has higher amounts of Ti and Fe, and PDI 11 more Cl. Moreover, none of the raw materials studied have a significant correlation with either of these two artefact samples. Group 2 is the only one where aluminium was detected, and also no correlation was established with the analysed geological materials. Group 3 differs from the others due to higher amount of calcium and lower of CO_2. Group 4 has the higher samarium and gadolinium contents. The group 5 has the higher potassium amounts, and high contents of magnesium. The sample PDI 13 has higher iron and manganese contents, and lower samarium contents. The vase analysed (PDV 7) has high content of H_2O, and low contents of titanium and Samarium, and has high boron content (Fig. 6.15).

Among geological samples, those from the nearby sources in the same "marble triangle" have chemical heterogeneities that make geochemical fingerprinting within them very challenging, as well as establishing correlations with artefacts. However, some correlations were possible to establish. For Groups 3, 4 and 5 artefacts the most likely source includes samples from the "marble triangle" Estremoz—Borba—Vila Viçosa, disregarding the Ruivina marble, which is the only one detachable from the others due especially to higher Si and lower Ca contents. The medium distance area sample—Tavira Breccia, like the latter, doesn't present any chemical affinity with the analysed artefacts. The remote area geological samples (MCE limestones—Moleanos, and Pêro Pinheiro—Lioz), don't seem to be a source for the artefacts, and LIOZ 2 is diverse from the others limestones. On the other hand, the vase PDV 7 is the only sample that has chemical similarity with a limestone sample, particularly the Moleanos 2 sample from MCE.

Among artefact samples no special correlation was established between the defined groups, and the respective archaeological contexts. Only samples PDI 10

and PDI 12 (Group 5) belong to the same context (pit 40), the other groups have artefacts from both "environment 1" and "pit 40" contexts. Unfortunately only one sample (PDV 7) was analysed from Sepulchral 1 context, and is also the only one pointing to a more remote source area.

6.3.3.4 The Achievements: Nearby and Long Distance Stone Procurement

Interpretations of the data may be used for general assessments of provenance, and PGAA became useful in distinguishing the various analysed artefacts revealing their diverse compositions, as well as being able to aid in the pointing to possible sources. A larger number of analyses may give more accurate results, especially for the geological materials. It is important to discuss the results obtained in a critical approach, taking into consideration that a more detailed geological survey and sampling are scheduled to be performed in the near future. Complementary analytical methods, including non-destructive ones are also planned to perform on both artefacts and geological material. Indeed, a larger number of geological samples may increase the accuracy of the predictions as well as make the indicated probability of provenance more realistic.

The stone artefacts at Perdigões show signs of both nearby and long distance procurement, as well as some of unknown attribution, as was already found for the ceramic materials (Dias et al. 2005). Among the stone materials, more than half (57 %) appear to have come from nearby, in particular from the marble triangle Estremoz-Borba-Vila Viçosa. Only one artefact definitely points to a long distance material source (in particular MCE limestones). The rest are from unknown sources.

Based on these results it would seem that imported foreign materials were used in parallel with regionally available materials. It is also interesting to notice that the object that points to the Lisbon peninsula limestones is of a different typological category (it is a vase) and was found in the tholoi tomb 1, which represents a different funerary procedure from that of the stone idols. So, different raw material provenances seem to be associated with different contexts and rituals, deepening the contrasts that we can see between these funerary features in Perdigões.

Besides provenance, one of the objectives of the study was to determine whether Prompt Gamma Activation Analyses (PGAA) could be successfully used to distinguish between marble/limestone samples originating from different known geological sources, as well as for matching artefacts to sources. It is important to emphasize that since the number of trace elements that can be measured by PGAA is restricted, also conclusions are limited, especially when dealing with such heterogeneous geological sources. Some of the present results might seem inconclusive; however, interpretations of the data may be used for general assessments of provenance.

6.3.4 *Distinguishing Style and Provenance of Ceramic Vessels*[4]

6.3.4.1 Summary of the Investigation

12 pottery fragments from the Inka Period (A.D. 1450–1532) Paria Basin, Bolivia were investigated by PGAA. One white sherd seemed to be foreign due to its different stylistic features (e.g. decorative motifs, paste). Based on their chemical composition it was possible to prove that 11 pots were manufactured from local raw material, while the white ceramic was non-local. In addition to its different style, the white pottery was formed from a raw material unknown in 30 km diameter circle around the archaeological site.

6.3.4.2 Standardized Inka Pottery: Imperial Ones and Resembling Others

This paper presents partial results of a comprehensive study, the Paria Archaeological Project (PAP 2004–2006), which—besides other topics—reconstructed the pottery handicraft of the Late Prehispanic Paria Basin of the Bolivian Altiplano (Condarco Castellón and Gyarmati 2012). As a result of the systematic surface survey carried out on a 95.5 km^2 area part of the Paria Basin in 2004 by the PAP, 113 sites ranging from the Formative Period (B.C. 1000–A.D. 600) until the Colonial Period (A.D. 1535–1825) were located. The most important and extended archaeological site of the basin is Paria, an Inka provincial administrative center (Gyarmati and Condarco Castellón 2014).

Pottery handicraft in the Inka Empire had a very characteristic pattern. As a part of the handicraft system, ceramic manufacturing was highly standardized. Hence, Inka Imperial pottery can be easily recognized through the whole Empire. Based on the archaeological record, it can be assumed that the Inka Imperial pottery manufacturing (1) was connected to certain workshops or (2) was assigned to strict conventions/regulations concerning the shape (categories were established by Meyers 1975, 1998; Matos n.d.), surface colour and treatment, and decorative motifs and their quality of the vessel. In this way, these items of the material culture could also express the strength and omnipotent aspect of the Empire (Fig. 6.16).

The majority of the Inka Period ceramic assemblage of the Paria Basin and the provincial center created during the Inka Period (A.D. 1450–1532) consisted of household pottery (various types of mostly undecorated or simple pattern painted pots, pitchers, and bowls used for storing liquids and raw foodstuffs, or for preparing food and beverages), and serving and storing vessels (jars, bowls, plates). According to their style, Inka Imperial, Inka imitation, mixed, local, and another

[4]Section written by Veronika Szilágyi.

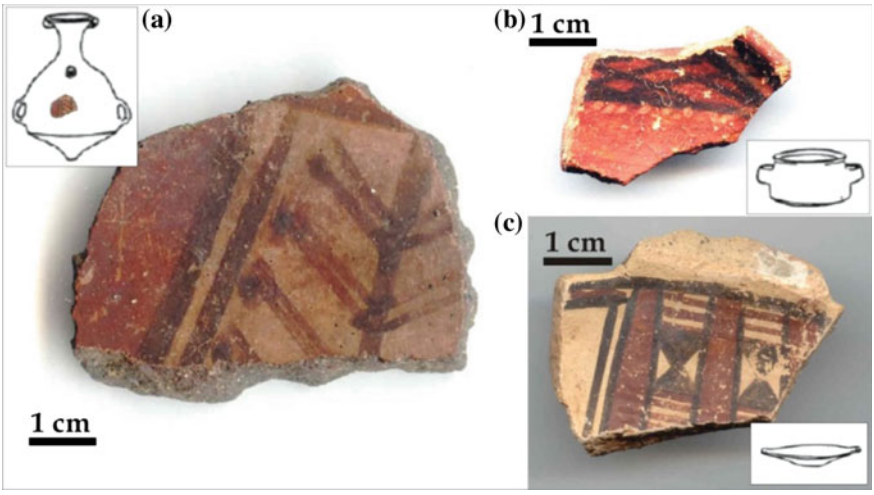

Fig. 6.16 Pottery fragments typical for the Inka Period assemblage of the Paria Basin. **a** No. PA/4, aribalo, Inka Imperial style; **b** No. BA/1, bowl, local style; **c** No. PA/5, plate, 'white pottery type'

style could be distinguished in the ceramic assemblage of the Paria Basin. The stylistic differentiation is based on a comprehensive macroscopic observation of form, quality and decoration. Inka Imperial style comprises vessels representing the best quality wares, and shapes and decorations are typical for the Inka culture. The Inka imitation style ceramics copy the Inka Imperial style vessels, but those are more poorly made and the decorations are less carefully executed. The mixed style blends the characteristics of the Inka and the Late Intermediate Period (in the following it is called Pre-Inka, A.D. 1100–1400). The local style is a ceramic type which survived from the Pre-Inka Period into Inka Period. The fifth stylistic group is represented by vessels which cannot be assigned either to the Inka or to the Pre-Inka pottery style. This group continues another Pre-Inka tradition that is foreign to the Paria Basin. It is typical for all the above mentioned five stylistic categories that the pots are red, orange, brown, grey or black on their surface, while they are entirely red or show sandwich structure in their profile.

'White pottery type' at Paria was made in the Inka Imperial style, decorated with motifs familiar from Cuzco polychrome pottery. This group incorporates bowls and plates of white, greyish white, or pinkish white body and sometimes of white slip. In terms of their shape, the whitish plates do not differ from the most common plate types made in the Inka Imperial style. Decorative elements are foreign to the altiplano (e.g. painted ulupica (*Capsicum cardenasii*) peppers, handle of a plate fragment modelled in the shape of a jaguar head).

Thus, we have to consider this 'white pottery type' as a member of the Inka Imperial style ceramic tradition but with a special manufacturing technology resulting in the white paste. It is an important question whether this technological

Table 6.3 Archaeological information and chemical data on the investigated Inka pottery fragments, and sedimentological information (gr. means granulometry) and chemical data on the comparative geological sample

Sample	BA/1	PA/1	PA/4	PA/6	P/12.13	P/12.17	P/12.20	P/34.143	P/53.79	P/63.7	P/92.4	PA/5	*SED-01*	*SED-02*	*SED-03*
Sample type	Pottery	Pottery	Pottery	Pottery	Pottery	Pottery	Pottery	Pottery	Pottery	Pottery	Pottery	Pottery	*Sediment*	*Sediment*	*Sediment*
Arch era	Inka	Inka	Inka	Inka	Inka-Col.	Inka-Col	Inka-Col.	Inka	Inka	Inka	Pre-Inka	Inka			
Style/*source*	Local	Inka Imp.	Inka Imp.	Inka Imp.	Inka Imit.	Inka Imp.	Inka Imp.	Inka Imit.	Inka Imit.	Inka Imit.	Local	'White'	*River bed*	*Terrace*	*Terrace*
Functional/*gr.*	Bowl	plate	Aribalo	Aribalo	Bowl	Plate	Plate	Bowl	Plate	Plate	Plate	Plate	*Fine sand*	*Fine sand*	*Fine sand*
Major elements (*wt%*)															
SiO_2	58.00	64.00	62.00	62.12	63.48	63.00	64.00	65.36	61.09	59.25	55.66	59.00	*77.00*	*75.00*	*88.00*
TiO_2	0.97	0.94	0.64	0.74	0.76	0.62	0.85	0.69	0.79	0.76	0.88	1.23	*0.53*	*0.60*	*0.34*
Al_2O_3	21.00	19.00	19.40	18.76	18.79	18.70	18.80	18.85	20.82	22.52	21.74	29.80	*10.20*	*10.60*	*4.70*
Fe_2O_3	7.10	6.70	4.80	4.99	5.37	5.10	6.70	5.46	7.04	7.20	6.40	2.50	*4.20*	*4.20*	*2.78*
MnO	0.19	0.114	0.064	0.06	0.12	0.084	0.081	0.04	0.10	0.10	0.06	0.03	*0.067*	*0.065*	*0.32*
MgO	2.50	2.00	2.20	1.67	2.28	2.00	1.90	1.88	2.07	2.12	2.39	0.70	*0.80*	*1.40*	*0.31*
CaO	2.60	0.38	1.90	2.19	2.90	1.40	1.00	0.98	1.16	1.12	2.74	0.34	*0.91*	*0.95*	*0.30*
Na_2O	1.86	1.01	2.13	2.30	1.40	2.51	1.29	1.11	0.88	0 85	2.00	0 83	*1.49*	*1.33*	*0.44*
K_2O	4.50	4.70	4.80	5.31	4.02	5.20	4.00	4.69	4 68	4.77	3.76	4.10	*2.41*	*2.52*	*1.13*
H_2O	1.07	1.28	2.145	1.74	0.79	1.40	0.81	0.82	1.27	1.22	4.23	1 49	*2.42*	*2.97*	*1.72*
Sum	99.79	100.12	100.08	99.88	99.91	100.01	99.43	99.88	99.90	99.91	99.86	100.02	*100.03*	*99.64*	*100.04*
Trace elements (*ppm*)															
Nd	52	59	55	76	49	36	53	43	41	36	67	80	*35*	*38*	*18*
Sm	5.7	9.7	5.8	6.5	5.6	5.8	5.9	5.1	5.7	5.4	7.0	8.9	*3.7*	*4.1*	*2.1*
B	94	91	109	118	149	143	117	205	136	130	104	125	61	93	74
Cl	154	60	350	400	78	430	600	295	86	94	582	32	69	400	95
Gd	6 4	9 0	6.0	6.0	6.0	5.0	6.8	5.1	6 4	6.2	6.4	10.6	4.2	4.9	2.8

trick is based on (1) the usage of a special raw material or (2) the introducing of a special firing technique. Comparison of the chemical composition of the 'white pottery type' with the classical Inka Imperial style vessel fragments can give answer to this problem.

The 12 pottery fragments investigated were found in the systematic surface survey of the PAP at different archaeological localities of the Paria Basin and from Inka Period context. According to the functional classification, these sherds belonged to plates-bowls or aribalos (narrow-necked jars similar to Roman amphorae) (see Table 6.3). One sample (No. PA/5) represents the 'white pottery type' described above, while other 11 sherds show stylistic features typical for the Inka Imperial, Inka imitation or the local style.

In addition to the archaeological samples, three comparative geological samples as potential raw materials were also subjected to PGAA. These samples were collected from the alluvial sediments of the Paria Basin.

In order to get a larger data set, comparative chemical data from an earlier investigation (Szilágyi et al. 2012) in the framework of the PAP was also utilized, as it is shown in Fig. 6.17. Those chemical concentrations were measured on archaeological and comparative geological materials by XRF and INAA.

6.3.4.3 Investigation of Pottery by PGAA: Is that a Good Choice?

PGAA seemed to be an effective analytical method for the chemical investigation of ceramics because of its non-destructive feature. Compared to other bulk chemical methods, it is possible to get the average composition without time-consuming

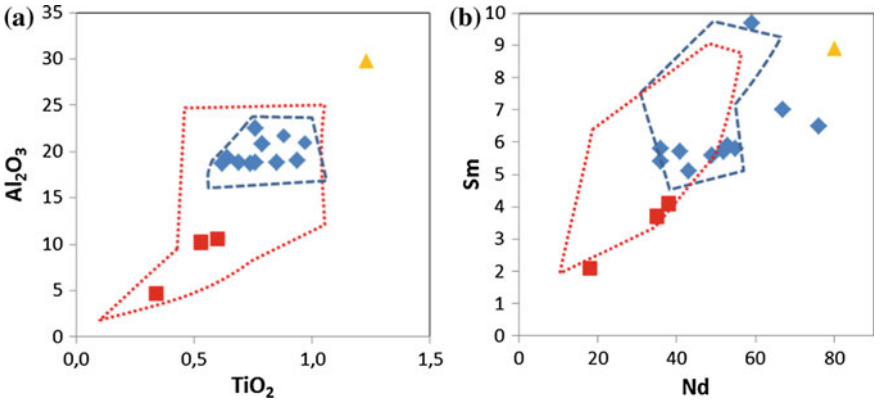

Fig. 6.17 Discriminating bivariate diagrams for **a** major-minor (TiO_2 vs. Al_2O_3) and **b** trace elements (**b**, Nd vs. Sm) (plotted concentrations are in wt% and μg/g). Inka ceramics measured by PGAA; ■ raw materials measured by PGAA; ▲ 'white pottery type' measured by PGAA; Inka ceramics measured by other methods (Szilágyi et al. 2012); raw materials measured by other methods (Szilágyi et al. 2012)

preparation of homogenized powder or fused bead. However, it is important to make sure that the irradiated volume of the sample does not contain any large-sized inhomogeneity (e.g. gravel-sized mineral/rock inclusion, thick decorative pigment layer, weathered layer, crack filled with secondary/post-burial phase). Since the neutron beam entirely penetrates the relatively thin and relatively light material of ceramics, it is not possible to separately measure the ceramic body (paste) and the surface layers (e.g. pigments, slips, glazes). Hence, it is important to know exactly which part of the pottery fragment was irradiated during the measurement. It will fundamentally determine the interpretation of the gained concentration data.

For example, the 12 pot sherds investigated here are 5 to 15 mm thick, and have <1 mm slip and/or <0.5 mm pigment layer on their surface. It is known that the pigments used are earth pigments and the slips are refined clayey suspensions. Hence, their composition is very similar to the ceramic body composed of clay minerals and other silicates. In addition, their quantity is almost negligible compared to the ceramic body. The applied collimations of the neutron beam were 10 mm^2, 24 mm^2, 1 cm × 1 cm and 1.41 cm × 1.41 cm. That means about 0.135 to 8.1 g (assuming a 2.7 g/cm^3 average density for ceramics) of the irradiated volume per sample. This mass is a representative amount to get information about the bulk chemical composition of the ceramic samples.

Another parameter to decide about is the optimal acquisition time per sample which was 3000–5000 s (live time) in the case of the 12 sherds investigated. Optimal time means long enough to get statistically reliable information (counts) in the spectrum, and as short as possible to save time. It is also conditioned by the counting rate which can be practically modified by collimation.

As an advantage, the range of elements measurable with PGAA (in this study—major: Si, Al, Fe, Mg, Ca, Na, K, H; minor: Ti, Mn; trace: Nd, Sm, Gd, B, Cl) can be more or less compared to other analytical methods (especially XRF) applied to another sample set of the Paria pottery assemblage (Szilágyi et al. 2012). Since the aim of the archaeometric study was to determine the provenance, the observed chemical elements were the geochemically immobile (partly incompatible) major, minor and trace elements. The oxides of the following major (SiO_2, Al_2O_3, partly Fe_2O_3) and minor elements (TiO_2, MgO), and trace elements (Nd, Sm and Gd) were considered. Immobile elements behave relatively constantly during the pottery manufacturing process (washing of the clay, tempering or mixing, firing) and the burial (leaching out or precipitation in soil solutions). Hence, these elements can show the initial/original chemical concentrations of the raw material even in the final product (i.e. pottery). As an experiment for ceramic archaeometric studies, other immobile trace elements (e.g. V, Cr, Co and Sc) would also be useful to be measured. Although, their detection is possible by PGAA, the quantification is possible only with large uncertainty. Another group of trace elements (e.g. other REEs, Th, U, Hf, Ta, As, Sb and Cs) cannot be successfully measured by PGAA but the data set can be easily completed with the help of INAA which is a conventional complementary method in trace element measurements.

6.3.4.4 From Chemical Data to Archaeological Interpretation

The 12 pot sherds investigated (belonging to Inka Imperial, Inka imitation and local styles) show a major element composition similar to an average argillaceous sedimentary rock (claystone, shale, siltstone). For comparison, see the PAAS (Post Archaean Australian Shale) which is a preferred standard material in geochemistry for fine-grained siliciclastic sediments (Nance and Taylor 1976; Taylor and McLennan 1985; McLennan 1989, 2001). The major element distribution for these sherds can be characterized with a moderate silica/alumina ratio (between 2.5 and 3.5), relatively high concentrations of specific cations in the silicate phases ($1.67 < MgO < 2.50$ wt%, $0.34 < CaO < 2.90$ wt%, $0.85 < Na_2O < 2.51$ wt%), while TiO_2 (between 0.62 and 0.94 wt%) and Fe_2O_3 (between 4.80 and 7.20 wt%) show lower concentrations compared to the average argillaceous sediments. Concerning the trace element distribution, Inka ceramics have relatively high concentrations of rare earth elements (REEs) ($36 < Nd < 76$ µg/g, $5.1 < Sm < 9.7$ µg/g, $5.0 < Gd < 9.0$ µg/g).

The major and trace element distribution of sample No. PA/5 (i.e. the representative of the 'white pottery type') is basically different from that of the other samples. The low silica/alumina ratio (1.98), the high TiO_2 (1.23 wt%) and average rare earth element content (Nd = 80 µg/g, Sm = 8.9 µg/g, Gd = 10.6 µg/g), and the low Fe_2O_3 (2.50 wt%), MgO (0.70 wt%) and CaO (0.34 wt%) content of the sample underlines a peculiar chemical character. This element distribution pattern quite differs from the average argillaceous sedimentary composition (i.e. PAAS). This supports the idea of a different geological origin of the 'white pottery type'. The enrichment of the TiO_2, Al_2O_3 and REEs can possibly indicate rather a metamorphic origin of the raw material (e.g. mica schist).

The three comparative fine-grained sand samples have much higher silica/alumina ratios (between 7.1 and 18.7) which reflect more sandy sediments than that of the raw material of the investigated ceramics. This characteristic affects the whole chemical element distribution of the samples, i.e. parallel with the higher SiO_2 concentration all other elements (especially TiO_2, Al_2O_3, MgO, K_2O, REEs) have lower concentrations than in the ceramic samples.

Figure 6.17 shows bivariate correlation diagrams of major (Fig. 6.17a, TiO_2 vs. Al_2O_3) and trace (Fig. 6.17b, Nd vs. Sm) elements of both the samples measured by PGAA and the data set published elsewhere (Szilágyi et al. 2012). Chemical data of Inka Imperial, Inka imitation and local style ceramics fit very well into the cluster outlined by the earlier data, although REEs show higher scattering by PGAA than by other methods. The three comparative fine-grained sand samples plot at the edge of the cluster outlined by the earlier data. It can be the result of the coarser grain size of the sand samples measured by PGAA, while the earlier work investigated clayey-silty sediments, too. Although, the three fine-grained sand samples could not act as real raw materials of the ceramics, it is clear that the cluster of the raw materials overlap with the cluster of the ceramics. In addition, the potential raw

material samples of the Paria Basin much rather similar to the Inka Imperial, Inka imitation and local style ceramics than to the 'white pottery type' which on both diagrams plots to the right upper corner.

Based on the chemical data of the investigated 12 pottery and the three sand samples, it can be assumed that the Inka Imperial, Inka imitation and local style ceramics of the Paria Basin and the provincial centre derived from local raw materials. The one representative of the 'white pottery type' seems to be foreign to the local sources of the Paria Basin regarding its chemical composition. Even if the comparison with the raw materials is extended to a data set collected from a 30 km circle around the archaeological site (Szilágyi et al. 2012), the above statement is correct.

6.3.4.5 Concluding Remarks

12 pottery fragments from the Inka Period Paria Basin, Bolivia were investigated by PGAA. One white sherd, though considered as member of the Inka Imperial style ceramic tradition, seemed to be manufactured with a special technology resulting in the white paste. Based on the chemical composition it was proved that one specialty of the technology was the usage of a special raw material (and not the application of a special firing technique). In addition, it was possible to establish that 11 pots were manufactured from local raw material, while the 'white pottery type' was non-local. Apart from its different style, the white pottery was formed from a raw material unknown in 30 km diameter circle around the archaeological site.

The statements of this study are established on the measurement of a single 'white pottery type' fragment. Even so, assuming that the same raw material was used for all the white coloured fragments (the pinkish hue can no doubt be attributed to the firing), vessels made in the Inka Imperial style but with white paste can be regarded as genuine imports. Moreover, almost 100 % of the ceramic assemblage of the Paria Basin and the provincial center created during the Inka Period had been manufactured locally, including the vessels previously considered as import wares from Cuzco (Gyarmati and Condarco Castellón 2014). 'White pottery type' as high prestige import wares, principally occur among the plates made in the Inka Imperial style used for consuming food.

The 176 analyzed sherds (Szilágyi et al. 2012; Szilágyi 2010; Gyarmati and Condarco Castellón 2014) included no more than nine bowl and plate fragments fired to a white or pink color made from a raw material not typical to the region. Although it was not possible to perform comparative analyses, the paste, decoration, and surface treatment of these vessels suggested that they had presumably been produced in the Milliraya state ceramic workshop (see Alconini 2013). Tschopik (1946) labelled this ware as Taraco Polychrome based on its primary distribution.

Fig. 6.18 Photo of the Eighteenth Dynasty (15th c. B.C.) Egyptian sealed pottery (Property of the Museum of Aquitaine in Bordeaux, France)

6.3.5 Looking Inside a Closed Egyptian Vessel[5]

A sealed pottery vessel originated from the Eighteenth Dynasty Egypt (15th c. B.C.) has been investigated using terahertz (THz) radiation, X-rays and neutrons. The vessel—among over 300 other objects found in pharaohs' graves—was bought by Dr. Jean Ernest Godard during his 1861 Egyptian mission. The object now belongs to the collection of the Museum of Aquitaine in Bordeaux, France (Saragoza 2008). A photo of the object can be seen on Fig. 6.18. A computed tomography with THz electromagnetic waves aimed to reveal its content non-destructively. Furthermore, owing to their higher spatial resolution and contrast, X-rays and neutrons were used to study its fabrication and conservation more precisely, together with the nature of its contents (Abraham et al. 2014). With neutron tomography, we were able to determine the method used to seal the jar, as well as the finer structure of the inner content. The investigations aimed to produce images with the help of neutrons—the methods have been discussed in Sect. 4.4. Applying a collimated beam of cold neutrons, elemental compositions of selected parts of the object were possible to determine. When

[5]Section written by Emmanuel Abraham, Maryelle Bessou, Zsolt Kasztovszky.

comparing the results of elemental analysis obtained from the void and full parts of the vessel, we can estimate the nature of the inner content, which was assumed to consist of dried germinated seeds (Abraham et al. 2014).

The neutron-based investigations of the Egyptian pottery have been performed at the NIPS-NORMA station of the Budapest Neutron Centre. On the basis of neutron radiography and tomography images taken at NIPS-NORMA, representative parts of the object have been chosen to determine their elemental composition. This method, which can save significant beamtime compared to the elemental mapping of the entire object, is called NR/NT-driven Prompt Gamma Activation Imaging (PGAI) (Kis et al. 2015). A cold neutron beam with a 2.7×10^7 cm^{-2} s^{-1} thermal equivalent flux has been collimated to 10×10 mm^2 area; the composition of selected parts have been analysed and semi-quantitative elemental compositions of each part were obtained. The acquisition time for each selected region of the PGAI measurement was set to 60,000 s. As neutrons travel through the whole body of the jar, they irradiate the wall of the jar, some void part, as well as the unknown inner content—in a chord-like volume.

Because of the special geometric arrangement of the different materials to be analysed, it was decided to irradiate the inner content together with the jar wall, as well as an irradiation of a part without filling material, which was performed separately (see Fig. 6.19). It would have needed a special measurement arrangement to analyse only the inner content from one single measurement. Unfortunately, collimating both the beam and the solid angle of the gamma detection would have significantly increased the acquisition time. Comparing the result of the two PGAA measurements, one can estimate the element composition for the inner content of the jar. Furthermore, the composition of the closure plug has also been determined similarly.

The elemental compositions of three different parts, determined by PGAI are given in Table 6.4. On Fig. 6.19, we indicate the parts where elemental analysis has been done marked with red boxes The investigated parts are the following: (i) ‘Full’: irradiation of the inner content and surrounding wall; (ii) ‘Void’: irradiation of a void part of the bottle without the filling material (e.g. practically only the wall material); (iii) ‘Plug’: irradiation of the closed neck region and surrounding walls. Since the geometry of the investigated sample is indefinite, and the efficiency and self-absorption corrections are uncertain, absolute concentrations of the identified chemical elements were not possible to obtain from the measured data. Instead, one can consider the results in Table 6.5, as a semi-quantitative identification of significant chemical elements. One can see that characteristic elements for ceramics (Na, Mg, Al, Si, K, Ca, Ti, Mn and Fe) are roughly in the same amounts in both ‘Full’ and ‘Void’ measurements, confirming the correctness of this approach. On the other hand, some elements characteristic of some organic material (H, C, N, S and Cl) show an excess in case of the ‘Full’ measurement, compared to the ‘Void’ one. Furthermore, the composition of the plug shows an excess of H, C, N, S and Cl too, which supports the organic nature of the string-like closure material.

As a result, we can finally conclude that the content could consist of germinated seeds (or any other dried organic material) such as barley which was a staple cereal

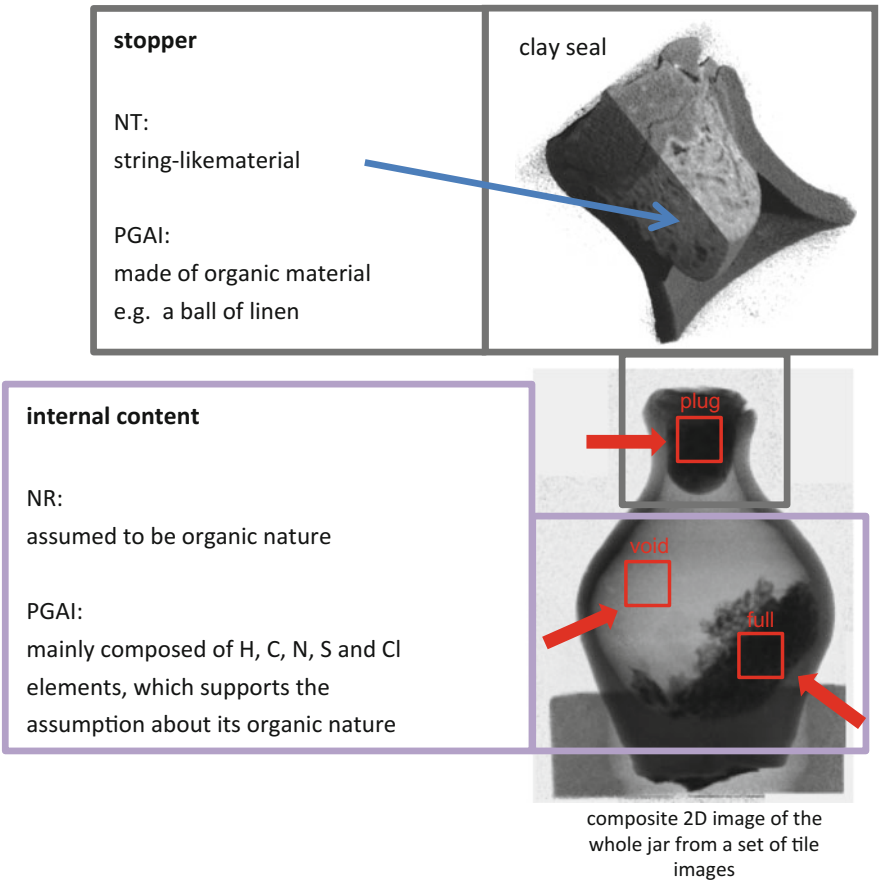

Fig. 6.19 Visualisation of inner parts of the sealed pottery by Neutron Tomography (NT) and by Neutron Radiography (NR); determination of composition by Prompt Gamma Activation Imaging (PGAI) at the Budapest Neutron Centre

Table 6.4 Composition of different parts of the sealed Egyptian pottery, measured by PGAI at the Budapest Neutron Centre

Full			Void			Plug		
El	wt%	*Rel. Unc. %*	El	wt%	*Rel. Unc. %*	El	wt%	*Rel. Unc. %*
H	1.3	*8*	H	0.4	*11*	H	1.4	*6*
B	0.0015	*8*	B	0.0016	*11*	B	0.0012	*6*
C	8.0	*11*	C	*<D.L.*		C	16.1	*8*
N	0.85	*10*	N	*<D.L.*		N	0.18	*23*
O	60.0	*5*	O	61.0	*7*	O	52.6	*6*
Na	0.89	*8*	Na	1.24	*11*	Na	0.95	*7*
Mg	1.3	*9*	Mg	1.6	*14*	Mg	1.2	*8*

(continued)

Table 6.4 (continued)

Full			Void			Plug		
Al	5.4	*8*	Al	6.3	*11*	Al	4.5	*7*
Si	14.4	*8*	Si	19.5	*11*	Si	13.2	*6*
S	0.046	*23*	S	*<D.L.*		S	0.14	*8*
Cl	0.058	*8*	Cl	0.033	*11*	Cl	0.18	*6*
K	0.93	*8*	K	1.05	*11*	K	0.66	*6*
Ca	2.2	*9*	Ca	2.3	*11*	Ca	4.5	*7*
Sc	0.0011	*8*	Sc	0.0006	*17*	Sc	0.0007	*7*
Ti	0.61	*8*	Ti	0.82	*11*	Ti	0.56	*7*
V	0.0082	*15*	V	0.016	*13*	V	0.012	*10*
Cr	0.039	*24*	Cr	0.042	*16*	Cr	0.017	*10*
Mn	0.071	*8*	Mn	0.098	*11*	Mn	0.065	*7*
Fe	4.0	*8*	Fe	5.6	*11*	Fe	3.6	*7*
Nd	0.0024	*15*	Nd	0.0032	*14*	Nd	0.0024	*11*
Sm	0.00042	*8*	Sm	0.00056	*11*	Sm	0.00034	*7*
Gd	0.00032	*10*	Gd	0.00046	*13*	Gd	0.00028	*9*

<D.L. means "less than the Detection Limit"

of Ancient Egypt. We also concluded with high confidence that the internal plug could be made of a ball of linen. Further investigation should consist in characterizing the molecular composition of these materials using a portable THz spectrometer in order to avoid the transportation of the fragile object and the use of a huge and costly instrument such as a research reactor.

6.3.6 *Small and Ultra Small Angle Neutron Scattering Investigation of Marbles*[6]

6.3.6.1 Description of the Investigated Artifacts

Investigations by means of SANS and USANS on marbles try to reveal a relationship between the mesoscopic structural evidences and the genetic conditions of the samples, known as the metamorphic process. This process consists on a isochemical evolution, depending on various parameters such as temperature and pressure, of a protolith, usually a a sedimentary carbonate with a highly variable calcitic–dolomitic composition, or a previous marble. It is characterized by the destruction of the originating minerals (mostly calcite—dolomite) followed by a further crystallization process. The metamorphic process proceeds through the progressive building up of structural units of increasing size: starting from

[6]Section written by Fabrizio LoCelso and Valerio Benfante.

elementary cells (nanometers, intermediate aggregates (micrometers), to the final crystals (millimeters) (D'amico et al. 1987). Here we show a selected group of white marbles, coming from several quarries in Northern Italy (Carrara, Elba, Musso, Campiglia) that have, despite their similar chemical composition, a different metamorphic history. The mesoscopic features will highlight their metamorphic evolution (the most important parameter is the temperature at which the process has taken place) within a rather confined geographical area, i.e. the Mediterranean basin, a region well known from the geological point of view.

6.3.6.2 Scientific Question

The use of SANS and USANS for fingerprinting white marbles originates from the fact the this material has been widely used, through the centuries, as a common building stone in monuments, statues and other objects of archaeological or cultural heritage interest. Numerous well known quarries are spread in the Mediterranean basin between Northern Italy and Greece, so it is clear that not only artistic and technological reasons move the archeologist but also the provenance and commercial routes that can testimony social contacts between different cultures. It has always been quite a challenge to identify the origin of white marbles (they look very similar at plain sight) and usually petrographic and isotopic analytical investigations have been used for fingerprinting purposes. These two techniques have surely well characterized the microscopic and macroscopic size domain while the scattering techniques will try to bridge the gap between the two, giving structural information on the mesoscopic regime. Indeed the combination of Small Angle Neutron Scattering (SANS) and Ultra Small Angle Neutron Scattering (USANS) allows indeed to obtain a way to interpret a possible link between the structure at mesoscopic level and the process that originates the marble, the metamorphic process. To this respect the thermal genetic characterization of the samples is a very important issue, since the temperature basically is the most important parameter in the history of a marble formation. In general, the maximum temperature involved in a metamorphic event can be calculated by using different mineralogical and geochemical geothermometers. For example trace minerals (silicates, etc.) acting as thermal markers, the solid solution of magnesite in the calcite lattice (Mg substituting for Ca), of iron sulphide into sphalerite (Fe substituting for Zn), which are in turn dependent on the crystallization temperature, the fluid inclusions which remain trapped in a number of crystals, and any eventual floating minerals, the isotopic fractionations concerning different mineral pairs (and nuclides): carbonate—carbonate (oxygen and carbon), carbonate–silicate or carbonate–oxide (oxygen). The petrographic investigation in the absence of the latter geothermometric information, can give an estimated metamorphic temperature by means of a simple observation (microscope with transmitted polarized light) of the marble in thin section (grain size, kind of aggregation, etc.).

6.3.6.3 Results

Geological materials are in general complex multiphase systems. However marbles, when investigated by means of neutron scattering, even if they are strictly multiphase they can be treated as a two phase system, as most of the scattering originates from the contrast between the inorganic components and the voids.

From the scattering theory we know that when a beam of neutrons radiation illuminates a volume V in which scattering centers (i.e. atoms and/or their aggregates) are distributed in real space (r) according to a distribution law ρ(r), scattering events take place and a scattered beam will be generated, whose coherent elastic differential scattering cross-section (often simply called scattering intensity) is related to the structure (distribution law ρ(r)), to the composition of the sample and to the scattering variable q ($q = 4\pi\sin\theta/\lambda$, where 2θ is the scattering angle and is λ the wavelength of the incident radiation). The form of this relationship depends on the degree of complexity of the structure present in the sample.

The scattering from geological systems has been described in terms of fractal structures (mass and/or surface fractals) and fractal exponents (Wong et al. 1986; Lucido et al. 1989, 1991). The possibility of extending the range of the scattering variable with the combined USANS and SANS techniques indeed allow a spatial resolution range of structural determination which can possibly reach about 30 mm in almost ideal conditions (Agamalian et al. 1997). The interpretation of scattering data from marbles, i.e. rocks originated from the building up of primary particles undergoing a continuous series of interaction processes mainly controlled by the metamorphic degree, depending mainly from the temperature (D'amico et al. 1987; Gorgoni et al. 2002) has been done with a rather simple model for describing fractal systems; a hierarchical structure model that takes into account the existence of a network of fractal aggregates of size R formed by monodispersed solid primary particles of radius r (Emmerling et al. 1994; Schmidt 1991).

The scattering intensity is therefore expressed as follows:

$$I(q) \propto P(q, r, D_s)S(q, r, D, R)$$

where

$$P(q, r, D_s) = \left(1 + \left(\sqrt{2}/3\right)\, q^2 r^2\right)^{0.5(Ds-6)}$$

and

$$S(q, r, D, R) = 1 + \left(D\Gamma(D-1)/qr^D\right)\left(1 + 1/qR^2\right)\sin[(D-1)\arctan(qR)]$$

$P(q, r, D_s)$ being the form factor referring to the single primary particle and $S(q, r, D, R)$ the structure factor that reflects the degree of order of primary particles along the aggregates (of size R). D_s is related to the dimensionality of the interfacial region of the primary particles, and its value must be between 2 and 3 ($D_s = 2$ is for smooth

particles following the Porod law $I \propto q^{-4}$). D is the power law exponent of the fractal aggregates.

Figure 6.20 (right column) shows schematically such a model (symbols are experimental data, the black solid line is the fit of the model to experimental data). At very low q the intensity is high and with tendency to level off; in other words, neutrons are probing length scales at which the system does no longer show any inhomogeneities and therefore it cannot be resolved. For larger values of q ($q > 1/R$) the scattering intensity drops because clusters of particles of radius R are being resolved; indeed it follows a power law characterized by the exponent D which is related to the fractal dimension or the branching of the aggregate. Going towards even larger q values it is possible to evaluate the radius r of the primary particles as well as D_s.

Based on the information available in the literature (Di Pisa et al. 1985; Cortecci et al. 1994; Pertusanti et al. 1993; Leoni and Tamponi 1991; Diella et al. 1992; Siletto et al. 1990), thermal ranges, related to the metamorphic process for the various samples were derived and reported in Table 6.5.

The results of the chemical analyses indicate that all samples are mainly calcitic, with only a minor, although variable, magnesitic (i.e. dolomitic) component. Such evidence is important in order to exclude any significant mesostructural effects to be eventually related to a highly variable crystal chemistry (i.e. variable calcitic–dolomitic composition). The thin section photographs reported in Fig. 6.20 (left columns), all taken at the same magnification for comparative evaluation, show the macroscopic structure of the samples. Their fabric is rather homogeneously granoblastic (i.e. homeoblastic) in almost all cases. Only sample A from Musso has a preferential orientation (i.e. lineation) of the tiny calcite grains forming the matrix in which a number of rather dispersed, larger crystals are included. Samples B and C from Carrara show a more markedly homogeneous fabric and very regular crystal boundaries, giving an overall polygonal to mosaic configuration. This is due to metamorphic equilibrium reached over very long time at the metamorphic temperature (Gorgoni et al. 2002). Generally speaking, the rough temperature—grain size correlation indicated above is confirmed by these pictures, with the exception of sample E. In fact, its high thermal range (500–600 °C, Table 6.5) is not consistent with the average grain size (0.25 mm), which is apparently indicative of a medium to medium-low metamorphic degree.

Parameters derived from the fits are reported in Table 6.5. It appears clearly that the radius r of the primary structural units increases homogeneously as a function of the thermal history of the samples, thus confirming the general control of the temperature on the dimension of the structural units. However, in the case of the scattering data, the correlation is perfectly shown by all the marbles analyzed, including sample E, meaning that the temperature–size relationship is better defined at the mesoscopic level compared to the macroscopic one. With the exception of sample A, the dimensionality of the interfacial region of the primary particles (D_s) roughly increases in the same direction, passing from 2 (very smooth surfaces) for the low and medium-low metamorphic degrees to around 2.3 for the higher grades. This would seem to indicate that the surface of these primary particles becomes

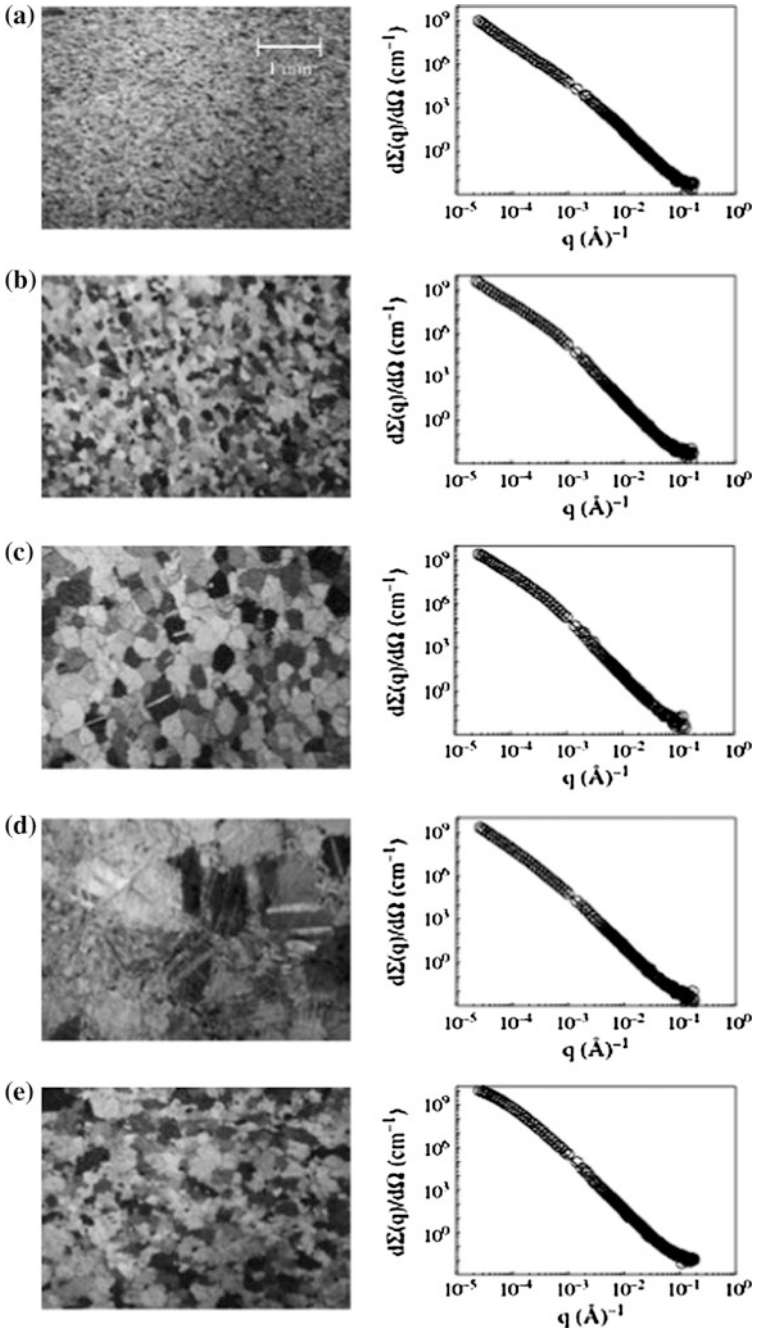

Fig. 6.20 Thin section photographs showing comparatively, at the same magnification, the macrostructural characteristics (i.e. fabric) of the marble samples (polarized light and crossed Nicols). Alongside are the corresponding measured neutron scattering cross sections

Table 6.5 The samples considered and analytical results from the fit for 5 different samples

Sample	Average grain size (mm)	Metamorphic degree (thermal ranges in °C)	D	r (Å)	10^3 D/r ($Å^{-1}$)	D_s
(A) Musso	0.05	Low (100–200)	2.50	2	1.225	2.45
(B) Carrara I	0.1	Medium-Low (200–300)	2.35	3.1	0.758	2
(C) Carrara II	0.35	Medium (300–400)	2.28	4.6	0.495	2
(D) Elba	1.5	Medium-High (400–500)	2.70	8.6	0.314	2.33
(E) Campliglia M.	0.25	High (500–600)	2.95	24	0.013	2.25

rougher with the increasing crystallization temperature. In such a context, it is interesting to notice that samples B and C from Carrara are the ones characterized by the smoothest possible surfaces of the structural units at both the meso- and macro-scale. The anomalously high Ds value for sample A could be explained by considering, in addition to the temperature, the effect of other parameters and features on the smoothness of the surface of the mesostructural units: (i) the amount (and kind) of fluids and the related control on the rheology of the system; (ii) the importance of time (at a given temperature) for the attainment of equilibrium or disequilibrium conditions, similarly to what is found at the macroscale level; and (iii) the possibility of a metamorphic evolution is more complex than usual, as already indicated. The situation for sample A from Musso is rather peculiar. On one hand, the prevailing matrix formed by very fine calcite crystals (Fig. 6.20a) is indicative of low crystallization temperatures (100–200 °C, Table 6.5). This anomalous feature has to be related to a rather complex evolutionary history, as indicated above, with special reference to the occurrence of those "retrograde phenomena" involving one or more further dynamometamorphic (low temperature) re-elaboration(s) of a previous higher grade marble, a process not unusual in the Alps, including this central-southern section (Diella et al. 1992; Siletto et al. 1990). Such an evolutionary complexity is probably responsible for a sort of memory

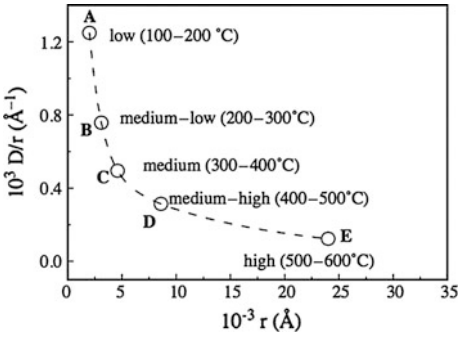

Fig. 6.21 D/r versus r plot for the five samples investigated, with indication of the corresponding metamorphic degree

effect. The relatively straightforward examination of the data already points out to a correlation between the fit parameters of the scattering data and the metamorphic conditions. As discussed above, the anomalies found hamper the use of simple correlation graphs, also on account of the limited (although representative) number of samples considered.

However, the binary correlation becomes much more significant when preceded by further processing of the data, i.e. by a normalization procedure. In particular, the D/r versus r correlation graph shown in Fig. 6.21 clearly indicates a hyperbolic trend, which can be easily explained considering the effect that the different metamorphic conditions have on the general mesostructural characteristics of the marbles analyzed.

6.3.6.4 Concluding Remarks Related to Marble Characterisation

A hierarchical structural model was used to analyze combined USANS—SANS patterns of white marble samples in order to relate their genesis with the features observed in the scattering experiments. By properly processing the fit parameters, we have been able to connect the characteristic parameters of the mesoscopic structure to the metamorphic evolution. In particular, the dimension r of the building units shows better correlation with the crystallization temperature than determined for the whole crystals at a macroscopic level. A similar but somewhat poorer correlation is found from aggregation (fractal dimension, D) and the surface characteristics (dimensionality of the interfacial region, D_s) of these intermediate clusters.

6.4 Final Thoughts

In the above examples, we have shown how neutron analytical methods can contribute to the research of tangible Cultural Heritage. In particular, a large number of specific questions regarding the provenance of objects can be answered with the help of analytical information (i.e. elemental- or isotopic composition, structure).

Obviously, during the investigations, any kinds of damage—neither visible nor invisible—are not allowed in case of valuable objects. Although a few methods, for instance the Instrumental Neutron Activation Analysis requires sampling of the objects, the rest apply external beam of neutrons, therefore large objects can be studied without sampling.

Furthermore, thanks to the low energy and relatively low intensity (10^7–10^9 cm^{-2} s^{-1}) of guided neutron beams, neutrons are perfect tools to study valuable and irretrievable objects of Cultural Heritage. Following the irradiation, no damage of the objects can be observed, and the induced radioactivity decays within a few days. The most common questions addressed the objects' provenance, i.e. the origin of its raw material, or the workshop or technique of its production. Sometimes, it is important to know whether the object is an original or a counterfeit. In fortunate instances many of these questions can be answered using non-destructive analytical methods.

Another advantage of using neutrons that neutron beam can penetrate into the sample, so as to supply analytical information from deeper regions of the objects. This feature is particularly advantageous if one intends to study the bulk composition of corroded metals, painted pottery or rocks with a layer of weathering. Certainly, the most comprehensive result can be obtained, when complementary 'surface' and 'bulk' methods are used simultaneously. Typical 'surface' methods that are applied in archaeometry: X-ray Fluorescence Analysis (XRF) and Proton Induced X-ray Emission (PIXE) analysis.

Finally, when a Cultural Heritage expert scheme a series of analytical investigations, he or she has to consider the availability and the cost/benefit ratios of various methods. Obviously, neutron based methods are usually realized on the basis of large scale facilities, such as research reactors or so called spallation sources (i.e. neutron sources maintained by collisions of accelerated protons on a heavy metal target). Both facilities are quite rare, only a few tens are available in the World. They are operated by a large number highly skilled staff. In addition, the operation of such facilities requires numerous safety issues. It follows that such methods are far not cheap, if one counts all the accessory costs of analysis. In principle, it is possible to operate mobile neutron analytical equipment, which uses radioactive neutron sources, but its efficiency is much lower than that of the large facilities. Many times, users of the Cultural Heritage research prefer to apply the easily available 'non-neutron based' methods, but sometimes the application of neutrons cannot be bypassed when valuable information is requested.

Acknowledgments The neutron-based experiments have been performed at the Budapest Neutron Centre, Hungary and at the FRMII, Germany. Most of the above mentioned research projects (the study of prehistoric stone objects, lapis lazuli, stone idols, the Egyptian vessel) have been performed using the financial support by the Transnational Access to Research Infrastructures activity in the 7th Framework Programme of the EU (CHARISMA Grant Agreement n. 228330).

The provenance study of prehistoric stone objects was also supported by the OTKA Hungarian Scientific Research Fund (Grant K 100385).

The archaeological project was carried out with the permission of the Dirección Nacional de Arqueología, Bolivia, and was financially supported by the OTKA Hungarian Scientific Research Fund (Grant T 047048), the Curtiss T. and Mary G. Brennan Foundation and the Heinz Foundation.

The colleagues from the Centre for Energy Research are thankful to Jesse L. Weil for the careful proofreading.

References

Abraham E, Bessou M, Ziéglé A, Hervé M-C, Szentmiklósi L, Kasztovszky Zs, Kis Z, Menu M (2014) Terahertz, X-ray and neutron computed tomography of an eighteenth dynasty Egyptian sealed pottery. Appl Phys A 117:963

Agamalian MM, Wignall GD, Triolo R (1997) Optimization of a Bonse-Hart ultra-small-angle neutron scattering facility by elimination of the rocking-curve wings. J Appl Crystallogr 30:345

Alconini S (2013) Chungara—Revista de Antropologia Chilena 45:2

Allmäe R, Limbo-Simovart J, Heapost L, Verš E (2012) The content of chemical elements in archaeological human bones as a source of nutrition research. Pap Anthropol XXI:27
Beltrán J, Loza Azuaga ML, Ontiveros Ortega E, Rodríguez Gutiérrez O, Taylor R (2012) The quarrying and use of Marmora in Baetica. An archaeometry-based research project. Italica 1:220
Biró K (2014) Carpathian obsidians: state of art. In: Lithic raw material exploitation and circulation in Préhistory. A comparative perspective in diverse palaeoenvironments, ERAUL, vol 138, p 47
Biró KT, Kasztovszky Zs (2009) In: Moreau JF, Auger R, Chabot J, Herzog A (eds) Proceedings of the 36th international symposium on archaeometry. Cahiers d'archéologie du CELAT, n. 25, Série archéométrie n. 7, p 143
Biró KT, Regenye J (1995) http://www.ace.hu/szentgal/
Blaise J, Cesbron F (1966) Données minéraliques et pétrographiques sur ke gisement de lapis-lazuli de Sare Sang. Bull Soc Fr Minér Cristallogr 89:333
Bourdonnec F-X, Delerue S, Dubernet S, Moretto P, Calligaro T, Dran J-C, Poupeau G (2005) PIXE characterization of western mediterranean and anatolian obsidians and Neolithic provenance studies. Nucl Instr Meth B 240:595
Buchanan B (1966) Catalogue of ancient near eastern seals in the ashmolean museum I, cylinder seals
Cann JR, Renfrew C (1964) The characterization of obsidian and its application to the mediterranean region. Proc Prehist Soc 30:111
Casanova M (1992) The sources of lapis lazuli found in Iran. In: Jarrige C (ed) South Asian archaeology 1989, p 49
Chakrabarti DK (1978) Human origins studies in India: position, problems and prospects. Man Environ 1–2:51
Condarco Castellón C, Gyarmati J (2012) An Reun Anu Etnol 23
Cortecci G, Leone G, Pochini A (1994) Stable isotope composition and geothermometry of metamphic rocks from the Apuane Alps, northern Tuscany, Italy. Miner Petrogr Acta 37:51
Crandell O (2012) Evaluation of PGAA data for provenance of lithic artifacts. Studia UBB Geologia 57(1):3
D'amico C, Innocenti F, Sassi FP (1987) Magmatismo e metamorfismo, Utet, Torino
Delmas AB, Casanova M (1990) The lapis lazuli sources in the ancient east. In: Taddei M (ed) South Asian archaeology 1987. Rome, p 493
Derakhshani J (1998) Die Arier in den nahöstlichen Quellen des 3. und 2. Jahrtausends v. Chr. Grundzüge der Vor- und Frühgeschichte Irans
Di Pisa A, Franceschelli M, Leoni L, Meccheri M (1985) Regional variation of the metamorphic temperatures across the Tuscan id I unit and its implications on the Alpine metamorphism (Apuan Alps, Northern Tuscany). Neues Jb Mineral 151:197
Dias MI, Prudêncio MI, Valera AC, Lago M, Gouveia MA (2005) Geoarch Bioarch Stud 3:161
Diella V, Spalla MJ, Tunesi A (1992) Contrasted thermo-mechanical evolutions in the Southalpine metamorphic basement of the Orobic Alps (Central Alps, Italy). J Metam Geol 10:203
Domínguez Bella S (2009) Huellas de cantería romana de mármol en Almadén de la Plata (Sevilla), un patrimonio a conservar. In: Nogales T, Beltrán J (eds) Marmora Hispana: explotación y uso de los materiales pétreos en la Hispania Romana, Roma, p 377
Emmerling A, Petricevic R, Wang P, Scheller H, Beck A, Fricke J (1994) Relationship between optical transparency and nanostructural features of silica aerogels. J Non-Cryst Solids 185:240
Faryad S (1999) Metamorphic evolution of the Precambrian South Badakhshan block, based on mineral reactions in metapelites and metabasites associated with whiteschists from Sare Sang (Western Hindu Kush, Afghanistan). Precambrian Res 98(3–4):223
Faryad SW (2002) J Petrol 43(4):725
Gebhard R, Wagner FE, Albert P, Hess H, Revay Z, Kudejova P, Kleszcz K, Wagner U (in preparation) J Radioanal Nucl Chem
Goldschmidth JR, Graff L, Joensu OI (1955) The occurrence of magnesian calcites in nature. Geochim Cosmochim Acta 1:212

Gorgoni C, Lazzarini L, Pallante P, Turi B (2002) In: Herrmann JJ, Herz N, Newman R (eds) Interdisciplinary studies on ancient stone. Archetype, London, p 115
Grew ES (1988) Nerupine at the Sar-e-Sang, Afghanistan, whiteschist locality: implications for tourmaline-kornerupine distribution in metamorphic rocks. KorAm Mineral 73:345
Gyarmati J, Condarco Castellón C (2014) Paria la Viexa. Pre-hispanic settlement patterns in the Paria Basin, Bolivia, and its Inka Provincial Center, Museum of Ethnography, Budapest
Herrmann G (1968) Lapis lazuli: the early phases of its trade. Iraq 30:21
Hogarth DD, Griffin WL (1978) Lapis Lazuli from Baffin Island, a Precambrian meta-evaporite. Lithos 11:37–60
Hurlbut CS (1954) Dana's manual of mineralogy, 17th edn. John Wiley & Sons Inc, New York
Kabaciński J, Sobkowiak-Tabaka I, Kasztovszky Zs, Pietrzak S, Langer JJ, Biró KT, Maróti B (2015) Transcharpatian influences in the Early Neolithic Poland. A case study of Kowalewko and Rudna Wielka Sites. Acta Arch Carp 50:5–32
Kasztovszky Zs, Antczak MM, Antczak A, Millan B, Bermúdez J, Sajo-Bohus L (2004) Provenance study of Amerindian pottery figurines with prompt gamma activation analysis. Nukleonika 49(3):107
Kasztovszky Zs, Biró KT, Markó A, Dobosi V (2008) Cold neutron prompt gamma activation analysis—a non-destructive method for characterization of high silica content chipped stone tools and raw materials. Archaeometry 50(1):12
Kasztovszky Zs, Biró KT, Szilágyi V, Maróti B, Težak-Gregl T, Burić M, Hágó A, Astalos C, Nagy-Korodi I, Berecki S, Hajnal A, Rácz B (2012) Abstracts of the 39th international symposium on archaeometry, Leuven, Belgium, 05.28–06.01
Kis Z, Szentmiklósi L, Belgya T (2015) NIPS–NORMA station—a combined facility for neutron-based nondestructive element analysis and imaging at the Budapest Neutron centre. Nucl Instr Meth A 779:116
Kostov R (2004) Roots of Bulgarian civilization. In: Academic interdisciplinary conference. Bul-Koreni, Sofia, p 77
Kramer SN (1952) Enmerkar and the Lord of Aratta: a Sumerian epic tale of Iraq and Iran. University Museum, University of Pennsylvania
Kulke HG (1976) Die Lapislazuli-Lagerstätte Sare Sang (Badakhshan). Afghanistan J 3(2):43
Lago M, Duarte C, Valera AC, Albergaria J, Almeida F, Carvalho A (1998) Povoado dos perdigoes (Reguengos de Monsaraz): dados preliminares dos trabalhos arqueologicos realizados em 1997. Rev Port Arqueol Lisboa 1(1):45
Lapuente P (1995) Mineralogical, petrographical and geochemical characterization of white marbles from Hispania. In: Maniatis Y, Herz N, Basiakos Y (eds) The study of marble and other stones used in antiquity, vol 151. London
Lapuente P, Turi B (1995) Marbles from Portugal: petrographic and isotopic characterization. Sci Technol Cult Herit 4(2):33–42
Leoni L, Tamponi M (1991) J Mineral Geochem 4:145
Lo Giudice A, Re A, Calusi S, Massi M, Olivero P, Pratesi G, Albonico M, Conz E (2009) Multitechnique characterization of lapis lazuli for provenance study. Anal Bioanal Chem 395:2211
Lucido G, Caponetti E, Triolo R (1989) Uso dei frattali in petrologia: esperimenti di scattering di neutroni ai bassi angoli su rocce magmatiche. Miner Petrogr Acta 32:185
Lucido G, Caponetti E, Triolo R (1991) Fractality as a working tool for petrology: small-angle neutron scattering experiments to detect critical behaviour of magma. Geol Carpath 42:85
Mañas Romero I (2012) Marmora de las canteras de Estremoz, Alconera y Sintra: su uso y difusión. In: García-Entero V (eds) El marmor en Hispania: explotación, uso y difusión en época romana, Madrid, p 331
Markó A, Biró KT, Kasztovszky Zs (2003) Szeletian felsitic porphyry: non-destructive analysis of a classical Palaeolithic raw material. Acta Arch Acad Scient Hung 54:297
Marschner H (1968) Ca-Mg-distribution in carbonates from the Lower Keuper in NW-Germany. In: Recent developments in carbonate sedimentology in Central Europe. Springer, Heidelberg, pp 128–135

Márquez JE, Valera AC, Becker H, Jiménez V, Suàrez J (2011) El complexo arqueológico dos Perdigões (Reguengos de Monsaraz, Portugal). Prospecciones Geofísicas—Campaña 2008–09, Trabajos de Prehistoria, Madrid
Martins R, Lopes L (2011) Mármores de Portugal. Rochas Equip 100:32
Matos M, Los Incas Arte y Simbolos (Banco de Crédito del Perú, Lima), p 109
McLennan SM (1989) In: Lipin BR, McKay G A (eds) Geochemistry and mineralogy of rare earth elements. Reviews in Mineralogy, vol. 21, p 169
McLennan SM (2001) Relationships between the trace element composition of sedimentary rocks and upper continental crust. Geochem Geophys Geosyst 2, 2000GC000109
Meyers A (1975) Algunas problemas en la Clasificación del estilo incaico, Puma-punku, vol 8
Meyers A (1998) Los Incas en el Ecuador análisis de los restos materiales. Quito, Abia-Yala
Molnár GL, Révay Z, Paul RL, Lindstrom RM (1998) Prompt-gamma activation analysis using the k_o approach. J Radioanal Nucl Chem 234:21
Molnár GL, Révay Z, Belgya T (2002) Wide energy range efficiency calibration method for Ge detectors. Nucl Instr Meth A 489:140
Moorey PRS (1994) Ancient mesopotamian materials and industries: the archaeological evidence. Clarendon Press, Oxford
Morbidelli P, Tucci P, Imperatori C, Polvorinos A, Preite Martinez M, Azzaro E, Hernandez MJ (2007) Roman quarries of the Iberian peninsula, Eur J Mineral 19(1):125
Nance WB, Taylor SR (1976) Rare-earth element patterns and crustal evolution. Geochim Cosmochim Acta 40:1539–1551
Oddone M, Márton P, Bigazzi G, Biró KT (1999) Chemical characterisations of Carpathian obsidian sources by instrumental and epithermal neutron activation analysis. J Radioanal Nucl Chem 240(1):147
Origlia F, Gliozzo E, Meccheri M, Spangenberg JE, Turbanti Memmi I, Papi E (2011) Mineralogical, petrographic and geochemical characterisation of white and coloured Iberian marbles in the context of the provenancing of some artefacts from Thamusida (Kenitra, Morocco). Eur J Mineral 23:857
Pertusanti PC, Raggi G, Ricci CA, Duranti S, Palmeri R (1993) Evoluzione post-collisionale dell'Elba centro-orientale. Mem Soc Geol Ital 49:297
Re A, Giudice AL, Angelici D, Calusi S, Giuntini L, Massi M, Pratesi G (2011) Lapis lazuli provenance study by means of micro-PIXE. Nucl Instr Meth B 269:2373–2377. doi:10.1016/j.nimb.2011.02.070
Révay Z (2006) Calculation of uncertainties in prompt gamma activation analysis. Nucl Instrum Meth A 564:688
Révay Z (2009) Determining elemental composition using prompt gamma activation analysis. Anal Chem 81:6851
Révay Z, Belgya T (2004) Principles of PGAA method. In: Molnár GL (ed) Handbook of Prompt Gamma Activation, Analysis with Neutron Beams. Kluwer Academic Publishers, Dordrecht, Boston, New York, pp 1–30
Révay Z, Belgya T, Ember PP, Molnár GL (2001a) Recent developments in hypermet-PC. J Radioanal Nucl Chem 248:401
Révay Z, Molnár GL, Belgya T, Kasztovszky Z, Firestone RB (2001b) A new γ-ray spectrum catalog and library for PGAA. J Radioanal Nucl Chem 248:395
Révay Z, Belgya T, Molnár GL (2005) New prompt k_0 and partial cross section values measured in the cold neutron beam of Budapest research reactor. J Radioanal Nucl Chem 265:261
Rómer F (1867) Első obsidian-Eszközök Magyarországon (in Hungarian) [First obsidian implements in Hungary]. Arch Közl 7:161
Rosen LV (1988) Lapis lazuli in geological and in ancient written sources. Partille, Sweden
Saragoza F (2008) Revue archéologique de Bordeaux, Tome IC, p 131 (French)
Sarianidi VI (1971) Archaeology Magazine 12
Schmidt PW (1991) Small-angle scattering studies of disordered, porous and fractal systems. J Appl Crystallogr 24:414

Schreyer W, Abraham K (1976) Three-stage metamorphic history of a whiteschist from Sar e Sang, Afghanistan, as part of a former evaporite deposit. Contrib Mineral Petrol 59:111
Searight S (2010) Lapis lazuli. In: Pursuit of a celestial stone. East and West Publishing Ltd., London
Siletto GB, Spalla MJ, Tunesi A, Nardo M, Soldo L (1990) Structural analysis in the Lario Basement (Central Southern Alps, Italy). Mem Soc Geol Ital 45:93
Szabó J (1867) A Tokaj-Hegyalja obsidiánjai (in Hungarian) [Obsidians of the Tokaj Mts]. A Magyarhoni Földtani Társulat Munkálatai (Pest) 3:147–172
Szakmány Gy, Kasztovszky Zs, Szilágyi V, Starnini E, Friedel O, Biró KT (2011) Discrimination of prehistoric polished stone tools from Hungary with non-destructive chemical Prompt gamma activation analyses (PGAA). Eur J Mineral 23:883
Szentmiklósi L, Belgya T, Révay Z, Kis Z (2010) J Radioanal Nucl Chem 286:501
Szilágyi V (2010) History of the Hungarian applied arts after 1945. Ph.D. thesis. Eötvös Loránd University of Budapest, Hungary
Szilágyi V, Gyarmati J, Tóth M, Taubald H, Balla M, Kasztovszky Zs, Szakmány Gy (2012) Petro-mineralogy and geochemistry as tools of provenance analysis on archaeological pottery: study of Inka period ceramics from Paria, Bolivia. J South American Earth Sci 36:1
Taelman D (2014) Contribution to the use of marble in Central-Lusitania in Roman times: The stone architectural decoration of Ammaia (São Salvador da Aramenha, Portugal), Archivo Espanol de Arqueologia, pp 175–194
Taelman D, Elburg M, Smet I, De Paepe P, Luís L, Vanhaecke F, Vermeulen F (2013) J Arch Sci 40(5):2227
Taylor SR, McLennan SM (1985) The continental crust: its composition and evolution. Blackwell Scientific Publications LTD, Oxford
Todd TW (1966) Petrogenetic classification of carbonate rocks. J Sediment Petrol 36(2):317
Tschopik MH (1946) Papers of the peabody museum of American archaeology and Ethnology 27(3)
Tykot RH (1997) Characterization of the Monte Arci (Sardinia) obsidian sources. J Archaeol Sci 24:467
Valera AC (2008) Cosmologia e recintos de fossos da Pré-História Recente: resultados da prospecção geofísica em Xancra (Cuba, Beja). Apontamentos de Arqueologia e Património, 7, Lisboa, Era Arqueologia, 8, Lisboa
Valera AC (2012a) In: Gibson A (ed) Mind the gap: Neolithic and Chalcolithic enclosures of South Portugal. Enclosing the Neolithic. Recent studies in Britain and Europe, BAR, p 165
Valera AC (2012b) In Gibaja JF, Carvalho AF, Chambom P (eds) Funerary practices from the mesolithic to the chalcolithic of the Northwest Mediterranean, British Archaeological Reports, p 103
Valera AC, Lago M, Duarte C, Evangelista LS (2000) Ambientes funerários no complexo arqueológico dos Perdigões: uma análise preliminar no contexto das práticas funerárias calcolíticas no Alentejo, Era Arqueologia, vol 2, Lisboa, Era/Colibri, p 84
Valera AC, Silva AM, Márquez Romero JEM (2014a) The temporality of Perdigões enclosures: absolute chronology of the structures and social practices, SPAL 23:11
Valera AC, Silva AM, Cunha C, Evangelista LS (2014b) In: Valera AC (ed) Recent prehistoric enclosures and funerary practices, vol 2676. BAR International Series, Oxford, pp 37–57
Vértes L, Tóth L (1963) Der Gebrauch des Glasigen quartzporphyrs im Paläolithikum des Bükk-Gebirges. Acta Arch Hung 15:3
Visy et al (eds) (2003) Hungarian archaeology at the turn of the Millennium, Nemzeti Kulturális Örökség Minisztériuma, Budapest
Webster M (1975) Gems, their sources, description and identification, London
Wong PZ, Howard J, Lin JS (1986) Surface roughening and the fractal nature of rocks. Phys Rev Lett 57:637

Woolley CL (1934) Ur excavations 2: the royal cemetery, Oxford
Yurgenson GA, Sukharev BP (1984) Localization conditions and mineral zoning of lazurite-containing bodies of Badakhshan. Zap Vses Min Obshch 113:498–505
Zöldföldi J, Kasztovszky Zs (2003) In: Hahn O, Goedicke C, Fuchs R, Horn I (eds) Proceedings of the international conference on archäometrie und Denkmalpflege. Universität Berlin, Berlin, p 194
Zöldföldi J, Kasztovszky Zs (2009) In: Maniatis Y (eds) ASMOSIA VII. Proceedings of the 7th international conference of association for the study of marble and other stones in antiquity. École française d'Athènes, Athenes, p 677